

# FIELD AND ACTION POTENTIAL RECORDINGS IN HEART SLICES: CORRELATION WITH ESTABLISHED *IN VITRO* AND *IN VIVO* MODELS

Herbert M. Himmel<sup>1\*</sup>, Alexandra Bussek<sup>3\*</sup>, Michael Hoffmann<sup>1</sup>, Rolf Beckmann<sup>1</sup>, Horst Lohmann<sup>2</sup>, Matthias Schmidt<sup>2</sup>, Erich Wettwer<sup>3</sup>

<sup>1</sup>Safety Pharmacology, Bayer HealthCare AG, Wuppertal, Germany;

<sup>2</sup>Lohmann Research Equipment, Castrop-Rauxel, Germany;

<sup>3</sup>Dept. of Pharmacology and Toxicology, Dresden University of Technology, Germany

\* These authors contributed equally to this work.

## Correspondence

Dr. Herbert M. Himmel, Safety Pharmacology Bayer HealthCare AG, Aprather Weg 18a D-42096 Wuppertal, Germany, phone +49-202-36-5108 (fax - 4755), e-mail [herbert.himmel@bayer.com](mailto:herbert.himmel@bayer.com)

## Key terms

Action potential, field potential, conscious dog, QT interval, cardiac repolarisation, hERG potassium current, hNav1.5 sodium current, ICH S7B, *in vitro* electrophysiological methods, papillary muscle, Purkinje fiber, rabbit Langendorff heart, heart slice

## Background and purpose

Action potential (AP) recordings in *ex vivo* heart preparations constitute an important component of the preclinical cardiac safety assessment according to ICH S7B guideline. Most AP measurement models are sensitive, predictive, and informative, but suffer from a low throughput. Here, effects of selected antiarrhythmics (flecainide, quinidine, atenolol, sotalol, dofetilide, nifedipine, verapamil) on field/action potentials (FP/AP) of guinea pig and rabbit ventricular slices are presented and compared with data from established *in vitro* and *in vivo* models.

## Experimental approach

Data from measurements of membrane currents (hERG, INa), AP/FP (guinea pig and rabbit ventricular slices), AP (rabbit Purkinje fiber (PF)), hemodynamic/ECG parameters (conscious, telemetered dog) are collected, compared and correlated to complementary published data (focused literature search).

## Key results

In the same concentration range, dofetilide inhibits hERG, and prolongs AP/FP duration in slices, and QTcV in dogs, whereas rabbit PF are about 10-fold more sensitive towards APD (AP duration) prolongation. These findings are corroborated by published data, and are observed in the range of human therapeutic plasma concentrations. Similar results are obtained for sotalol. Nifedipine lowers blood pressure and increases heart rate without prolonging but slightly shortening QTcV in dogs. Shortening of FPD / APD in slices and rabbit PF are observed at similar nifedipine concentrations, consistent with the literature. These are, however, higher than those required for ICaL inhibition (~10-fold) and hemodynamic effects (>100-fold). Atenolol prolongs the PQ interval in dogs at human therapeutic plasma concentrations, but does not markedly alter FPD / APD in slices and rabbit PF, and QTcV in dogs. Flecainide hardly alters FPD / APD in slices, and rabbit PF, despite its potent hERG inhibition. QTcV in dogs remains unaffected. In the same concentration range, flecainide inhibits INa, hence slows AP upstroke in rabbit PF and slice preparations, and widens QRS complex in dogs, thus confirming published data.

AP, action potential; APA, AP amplitude; APD, AP duration; BDM, 2,3-butanedione monoxime; DMSO, dimethylsulfoxide; ECG, electrocardiogram; FP, field potential; FPD, FP duration; HEK, human embryonic kidney; hERG, human ether-a-go-go-related gene; HK+ solution, high potassium solution; ICaL, L-type Ca<sup>2+</sup> current; INa, Na<sup>+</sup> current; PF, Purkinje fiber; PM, papillary muscle; QNa, latency difference between primary and secondary peak of the FP as measure for Na<sup>+</sup> conductance; QTcV, QT interval corrected for heart rate according to Van de Water; RMP, resting membrane potential; V<sub>max</sub>, maximal AP upstroke velocity

### *Conclusion and implications*

FP/AP recordings from guinea pig and rabbit heart slices are affected by selected antiarrhythmics in a similar manner as in established *in vitro* and *in vivo* models. This pharmacological correlation and thus predictability of effects might render heart slice preparations advantageous, because of their potential of enhanced throughput and opportunity to reduce use of laboratory animals.

## **Introduction**

Although action potential (AP) recordings in *ex vivo* heart preparations are not a requirement within the framework of the ICH S7B guideline for the cardiac safety of drugs (Anon, 2005), they still constitute an important component of the preclinical cardiac safety assessment of new chemical entities, because AP recordings provide the electrophysiologist with a wealth of information. While most AP measurement models, e.g. papillary muscle, Purkinje fiber, ventricular strips, etc. are sensitive, predictive, and informative, they usually suffer from a low throughput. One promising approach to overcome this limitation constitutes the synchronous recording of bioelectrical signals from multiple cardiac tissue slices, a technique which has been recently optimised (Bussek et al., 2009). Here, effects of selected Class-1 to -4 antiarrhythmics on field and action potentials (FP, AP) of guinea pig and rabbit ventricular slices are presented and compared with established *in vitro* and *in vivo* models.

Tissue slices from brain, kidney, liver, lung, and pancreas are well established models for electrophysiological, biochemical, and toxicological studies (Edwards et al., 1989; Parrish et al., 1995; Vickers and Fisher, 2004; Colbert, 2006). Compared with isolated cells, e.g. cardiomyocytes, tissue slices offer the advantages of preserved tissue structure, no enzymatic digestion, no selection of cells during the isolation procedure, no exposure to alien growth factors or serum, and viability for considerable periods of time when maintained under appropriate conditions. While isolated cardiomyocytes allow numerous measurements in cells from a single heart, the lack of intercellular contacts or cell surface damage by enzymatic digestion may lead to erroneous conclusions about drug actions. On the other hand, pharmacological and electrophysiological experiments in Langendorff hearts, papillary muscle or Purkinje fibers provide evidence of drug action under conditions more or less close to *in vivo* physiology, but are time-consuming and expensive, because only a limited number of drugs or drug concentrations can be tested in the heart of one animal. Heart slices combine the advantages of whole organ and isolated cells, because they exhibit intact tissue structure and cellular contacts, yet a large number of preparations is obtained from a single heart. Furthermore, the slice thickness (350 µm) ensures maintained tissue oxygenation which may become limiting in other *in vitro* heart preparations like papillary muscles (Barclay, 2005).

In this paper, we present integrated data on the electrophysiological effects of selected antiarrhythmic drugs (flecainide, quinidine, atenolol, sotalol, dofetilide, nifedipine, verapamil) using complementary *in vitro* and *in vivo* approaches. The experimental techniques range from measurement of membrane currents (hERG, I<sub>Na</sub>, I<sub>CaL</sub>), to action/field potentials in slices, Purkinje fiber APs, and hemodynamic/ECG parameters in conscious, telemetered Beagle dogs, and also include published data. The main result of this complementary approach is that FP/AP recordings from heart slices correlate well with established *in vitro* and *in vivo* models in terms of pharmacology and predictability. Heart slice preparations yield similar results as papillary muscles, but offer enhanced throughput for mechanistic investigations, and may substantially reduce the use of laboratory animals. This work has been presented previously at the annual meeting of the Safety Pharmacology Society (Sept. 2010, Boston, MA, USA).

## Methods

### Drugs

Chemicals and drugs (flecainide acetate [Flecainid-Isis® tablets], quinidine hydrochloride monohydrate, atenolol, dofetilide, D,L-sotalol hydrochloride [Sotalol ratiopharm® tablets], nifedipine, verapamil hydrochloride) were provided by Bayer-Schering Pharma or obtained from commercial sources (Sigma-Aldrich; RBI; local pharmacy) and stored at room temperature or as appropriate. On each of the experimental days, drug solutions were freshly prepared using frozen stock solutions (in DMSO) for *in vitro* studies. For *in vivo* studies (oral administration of gelatine capsules, 0.25 mL kg<sup>-1</sup>), drugs were formulated in water (verapamil), aqueous Tylose MH300 (0.5 %; atenolol, dofetilide), ethanol / polyethylene glycol 400 (PEG400, 10:90; quinidine), PEG400 (nifedipine), or as pulverised tablets in gelatine capsules (flecainide, D,L-sotalol). Solutions and formulations were stored at room temperature.

Drug/molecular target nomenclature (e.g. receptors, ion channels, etc) follows and conforms to BJP's Guide to Receptors and Channels (Alexander et al., 2009).

### *In vitro* electrophysiology studies: hERG K<sup>+</sup> current

HEK (human embryonic kidney) 293 cells stably transfected with cDNA encoding the hERG (**h**uman **e**ther-**a**-**g**o-**g**o-**r**elated **g**ene) K<sup>+</sup> channel (Zhou et al., 1998) were cultured as previously described (Himmel, 2007). The single electrode whole cell voltage clamp method was applied using an EPC-9 amplifier and TIDA 5 software (HEKA Elektronik, Lambrecht, Germany) at room temperature as previously reported (Himmel, 2007).

The clamp protocol consisted of stepping the command voltage to +20 mV (duration 1000 ms) followed by a hyperpolarizing step to -120 mV (500 ms) and a step back to the holding potential of -80 mV (cycle length 12 s). The inward tail current elicited by stepping from +20 mV to -120 mV was used to quantify hERG K<sup>+</sup> current.

The standard extracellular solution was composed of (in mM): NaCl 146.0, KCl 4.0, CaCl<sub>2</sub> 2.0, MgCl<sub>2</sub> 2.0, HEPES 10.0 (pH 7.4; 300-310 mosmol l<sup>-1</sup>). The intracellular (electrode filling) solution was composed of (in mM): KCl 135.0, MgATP 2.0, HEPES 10.0, EGTA 10.0 (pH 7.4; 290-300 mosmol l<sup>-1</sup>).

The concentration dependence of effects was modelled with a standard four-parameter logistic equation:  $\text{effect} = \text{min} + \frac{\text{max}}{1 + 10^{((\log\text{IC}_{50} - \log X) * nH)}}$ , with minimal and maximal effects (min, max), half-maximal inhibitory drug concentration (IC<sub>50</sub>), drug concentration (X), and Hill slope (nH). Minimal and maximal effects were usually treated as constants (max = 100 and min = 0), and IC<sub>50</sub> and nH as variables (GraphPad Prism 3).

### *In vitro* electrophysiology studies: hNav1.5 Na<sup>+</sup> current

HEK 293 cells stably transfected with cDNA encoding the hNav1.5 Na<sup>+</sup> channel were cultured under standard conditions (Section 2.2; Himmel and Hoffmann, 2010). The clamp protocol (whole cell voltage clamp, 22°C) consisted of stepping the command voltage to -120 mV (duration 500 ms) followed by a depolarising step to -35 mV (20 ms) and a step back to the holding potential of -80 mV (cycle length 2 s). The peak inward current elicited by stepping from -120 mV to -35 mV was used to quantify hNav1.5 Na<sup>+</sup> current. The bath solution consisted of (mM) NaCl 150, KCl 2, MgCl<sub>2</sub> 1, CaCl<sub>2</sub> 1.5, HEPES 10, glucose 5 (pH 7.4); the pipette solution contained (mM): KCl 35, CsF 105, EGTA 10, HEPES 10 (pH 7.4).

### *In vitro* electrophysiology studies: rabbit Purkinje fiber action potential

Purkinje fibers were carefully dissected from the ventricles of female rabbit hearts (strain: New Zealand White and Chinchilla; age 4-14 months; body weight 2-5 kg) and stored in high-K<sup>+</sup> Tyrode solution at 37°C as previously described (Vormberge et al., 2006; Himmel, 2007). Purkinje fibers were mounted in a horizontal organ bath that was perfused in a non-circulating manner with oxygenated (95% O<sub>2</sub>, 5% CO<sub>2</sub>) standard recording Tyrode solution (3 ml/min; 37°C). The recording Tyrode solution was composed of (in mM) NaCl 127.0, KCl 3.0, CaCl<sub>2</sub> 1.8, MgCl<sub>2</sub> 0.5, NaH<sub>2</sub>PO<sub>4</sub> 0.36, NaHCO<sub>3</sub> 22.0, D(+)-glucose 5.5 (pH 7.4 ± 0.1 at 37 ± 1°C following equilibration with 95% O<sub>2</sub>, 5% CO<sub>2</sub>). The preparations were stimulated electrically by means of square wave pulses (duration: 2 ms; 50% above threshold) at a standard stimulation rate of 1 Hz (software ISO-2, MFK, Niedernhausen, Germany). Conventional borosilicate glass microelectrodes with tip resistances of 20-40 MΩ when filled with 3 M KCl were used in order to measure action potentials (APs) intracellularly with a microelectrode amplifier (model BA-1S, npi electronic, Tamm, Germany).

Each preparation was equilibrated in the bath for approximately 60 minutes. When the impalement was stable, the bath was perfused with drug solution at cumulatively increasing concentrations (30 minutes per concentration) followed by washout. The frequency dependence of effects was assessed by varying the stimulation frequency (0.2, 1.0, and 2.5 Hz).

Digitally recorded (10 kHz) APs were analysed for resting membrane potential (RMP), AP amplitude (APA), maximal upstroke velocity (V<sub>max</sub>), plateau potential at 35 ms after the upstroke, and AP duration at 50% and 90% of repolarisation (APD<sub>50</sub>, APD<sub>90</sub>). Furthermore, the ratio of APD<sub>50</sub> divided by APD<sub>90</sub> was calculated in order to quantify the potential AP triangulation.

### *In vitro* electrophysiology studies: guinea pig papillary muscle action potential

Papillary muscles were dissected from the ventricles of female guinea pig hearts (strain: Dunkin Hartley; body weight 200-250 g). Papillary muscles were mounted in a horizontal organ bath that was perfused in a non-circulating manner with oxygenated (95% O<sub>2</sub>, 5% CO<sub>2</sub>) Tyrode solution (35°C). Conventional borosilicate glass microelectrodes (20-40 MΩ, 3 M KCl) were used in order to measure APs at 1 Hz (software ISO-2, MFK, Niedernhausen, Germany) with a microelectrode amplifier (model BA-1S, npi electronic, Tamm, Germany).

Each preparation was equilibrated in the bath for approximately 60 minutes. When the impalement was stable, the bath was perfused with D,L-sotalol or quinidine at cumulatively increasing concentrations (30 minutes per concentration). The frequency dependence of effects was assessed by varying the stimulation frequency (0.3, 1.0, and 3.0 Hz).

Digitally recorded APs were analysed for resting membrane potential (RMP), AP amplitude (APA), maximal upstroke velocity (V<sub>max</sub>), and AP duration at 30, 60 and 90 % of repolarisation (APD<sub>30</sub>, APD<sub>60</sub>, APD<sub>90</sub>).

### *In vitro* electrophysiology studies: guinea pig and rabbit left ventricular slice action and field potentials

Ventricular heart slices were obtained from male guinea pigs (about 300 g body weight; Charles River, Sulzfeld, Germany) and female rabbits (strain: chinchilla; 2.0 - 2.5 kg body weight; Charles River, Sulzfeld, Germany) as described previously (Bussek et al., 2009). Briefly, animals were anaesthetised (guinea pig: 70% CO<sub>2</sub>, 30% O<sub>2</sub>; rabbit: ketamine/xylazine 50/12 mg/kg i.m. and 10/5 mg/kg i.v.) and their hearts were quickly removed and perfused on a Langendorff apparatus with oxygenated (5% CO<sub>2</sub>, 95% O<sub>2</sub>) Tyrode's solution (composition in mM: NaCl 126.7, NaH<sub>2</sub>PO<sub>4</sub> 0.4, NaHCO<sub>3</sub> 22, KCl 5.4, CaCl<sub>2</sub> 1.8, MgCl<sub>2</sub> 1.1, glucose 5, pH 7.4) for 1 minute followed by a 1 minute

perfusion with high potassium ( $\text{HK}^+$ ) solution (composition in mM: NaCl 120, KCl 20,  $\text{CaCl}_2$  2,  $\text{MgCl}_2$  1, HEPES 10, glucose 10, pH 7.4) to inhibit electrical activity. Contractile activation was suppressed with 2,3-butanedione monoxime (BDM, 15 mM; [Sellin and McArdle, 1994](#)).

A tissue piece (10 x 4 mm) of the middle part of the left ventricle was glued directly to an agarose block with histoacryl tissue adhesive (Aesculap AG & Co. KG, Tuttlingen, Germany), with the tissue position corresponding to the slice direction. This procedure allows direct contact between the heart tissue and the superfusion solution in order to avoid the risk of inadequate oxygen supply. The block was then fixed to the cutting stage of a vibratome (Integraslice, Campden Instruments Ltd., Loughborough, UK). Vertical transmural slices (consisting of epi-, midmyo-, and endocardial layers) of 350  $\mu\text{m}$  thickness were cut in cold ( $4^\circ\text{C}$ ) oxygenated  $\text{HK}^+$  solution containing 15 mM BDM. Cutting was done with a steel blade driven at a speed of  $0.03 \text{ mm}\cdot\text{s}^{-1}$ , amplitude of 1 mm and vibration frequency of 51 Hz. Freshly prepared slices were stored in oxygenated  $\text{HK}^+$  solution at room temperature, and fixed by a grid ("slice holder", SDH-27N/15, Harvard Apparatus, Holliston, MA, USA).

To characterise the electrophysiological parameters of guinea pig and rabbit cardiac slices, we recorded extracellular field potentials (FPs) and intracellular action potentials (APs) in the mid-myocardium at the center of the slices. Myocardial slices were transferred to a 4-channel submerged type recording chamber (Lohmann Research Equipment (LRE), Castrop-Rauxel, Germany) and continuously superfused with oxygenated Tyrode's solution ( $2 \text{ ml min}^{-1}$ ) at  $37^\circ\text{C}$ . Field potentials (FP) were recorded simultaneously in up to 4 heart slices using the multiple slice evaluation system Synchronslice (LRE, Castrop-Rauxel, Germany). Concentric bipolar stainless steel stimulation electrodes (LRE; diameter 1.5 mm), used in order to minimise effects of stimulation on neurotransmitter release, and tungsten platinum recording electrodes (Thomas Recording, Giessen, Germany) were advanced until contact with the slice surface using manually driven micromanipulators under visual control through a multiple CCD camera system. Data acquisition (sampling rate 10 kHz per channel, bandwidth 1 Hz - 3 kHz), electrical stimulation (1 Hz), and application of drugs to the superfusion with an 8-channel Teflon valve system were controlled via automated software (SynchroHeart, LRE). The software was also used for offline analysis of single FP component amplitudes, slopes, and latencies. In addition, the difference between the primary (positive or negative) and secondary (negative or positive) peak latencies, termed QNa, were analysed in order to detect changes in  $\text{Na}^+$  conductance.

Intracellular action potentials were recorded with conventional glass micropipettes ([Bussek et al., 2009](#)). Signals were accepted when the resting membrane potential was more negative than -75 mV and the amplitude of the action potential was larger than 115 mV. After 40 min under control conditions, drugs were cumulatively added (one concentration every 30 min) to the superfusion solution.

## Cardiovascular function and ECG in conscious dogs *in vivo*

The animal care and experimental procedures were in accordance with the German Law on the Protection of Animals and were performed with the permission from the State Animal Welfare Committee. Furthermore, all dogs were examined prior to the experiments and found to be healthy. Beagle dogs of either sex (body weight: 11–20 kg, age: 2–8 years) were obtained from various commercial breeders. The dogs were identified by a tattooed ear number and a collar and housed in groups of 2-3 animals. Lights were on for 12 hours per day from 6 a.m. to 6 p.m., room temperature was  $20\text{--}23^\circ\text{C}$ , and relative humidity 30-70 %. The dogs were fed once daily with pelleted standard dog chow, drinking water was available ad libitum.

Briefly, under general anaesthesia the dogs were implanted with a telemetry device (model TL11M2-D70-PCT; Data Science Inc. (DSI), St. Paul, MN, USA) comprising a transmitter, a catheter and two electrodes. The body of the transmitter was inserted into a subcutaneous pouch made on the dog's

flank. The catheter was passed subcutaneously to the femoral artery, inserted distal to the inguinal ligament, and advanced approximately 20 cm upstream to measure blood pressure in the abdominal aorta. The two ECG electrodes were placed subcutaneously in a standard lead II configuration. After the implantation surgery, a postoperative recovery of at least 2 weeks was allowed.

For measurement of blood pressure and ECG, the dogs were separated into a cage equipped with 2 individual telemetry receivers (model RMC-1, DSI). The signals were captured using Ponemah P3 Plus software (V.4.10 including Dataquest OpenART, V.2.30, DSI). Collected data was averaged over a period of 15 minutes, and telemetry signals were analysed for systolic, diastolic and mean arterial blood pressure, heart rate, and various ECG intervals (PQ, QRS, QT, QTc). QT intervals were corrected for heart rate according to van de Water (QTcV; [van de Water et al., 1989](#)).

Data collection began at least 90 minutes before administration of either of the test compounds. Following drug administration at 3:30 p.m., data was recorded overnight for a period of about 15 hours. Drug effects were assessed as the changes versus predrug values as compared to those of the vehicle control group.

## Determination of drug plasma concentrations in dogs

Blood samples for determination of drug plasma concentrations were taken from satellite animals of either sex without telemetry implant (N=3-4 per group) via the jugular vein or cephalic vein into lithium-heparin coated monovettes at 1, 3, 7, and 24 hours post-treatment. After centrifugation at  $\leq 4^{\circ}\text{C}$ , the plasma samples were stored at  $-20^{\circ}\text{C}$  until analysis. Following protein precipitation with acetonitrile or acetonitrile/ammonium acetate including an appropriate internal standard, drug concentrations in plasma were determined by means of high-pressure liquid chromatography (HPLC) and tandem mass spectrometry detection. In case of D,L-sotalol determination, plasma concentrations were measured after solid phase extraction using separation by HPLC and fluorescence detection. Lower limits of quantitation were  $0.25 \mu\text{g l}^{-1}$  for flecainide, quinidine, dofetilide, and verapamil,  $0.5 \mu\text{g l}^{-1}$  for nifedipine,  $5 \mu\text{g l}^{-1}$  for atenolol, and  $12 \mu\text{g l}^{-1}$  for D,L-sotalol.

## Statistics

The data reported are rounded group mean values and corresponding standard deviation (SD) of N experiments unless indicated otherwise. Statistical analysis was performed either as ordinary one-way or repeated measures ANOVA followed by Dunnett's multiple comparisons post-hoc test or by applying an appropriate nonparametric test. Differences were considered statistically significant if  $p < 0.05$ . Statistical analysis and graphical presentation of data was done with GraphPad Prism (release 3) or Microsoft Excel.

## Focused literature search

A literature search in PubMed (<http://www.ncbi.nlm.nih.gov/pubmed/>) was conducted using the terms flecainide, quinidine, atenolol, sotalol, dofetilide, nifedipine, verapamil, antiarrhythmic, hERG, calcium channel, sodium channel, action potential, Purkinje fiber, papillary muscle, ECG, QT/QTc, QRS, plasma concentration either alone or in various combinations. Among the numerous retrieved articles, we focused on those presenting concentration-effect data *in vitro* and *ex vivo*, and dose dependence of effects together with exposure data *in vivo*.



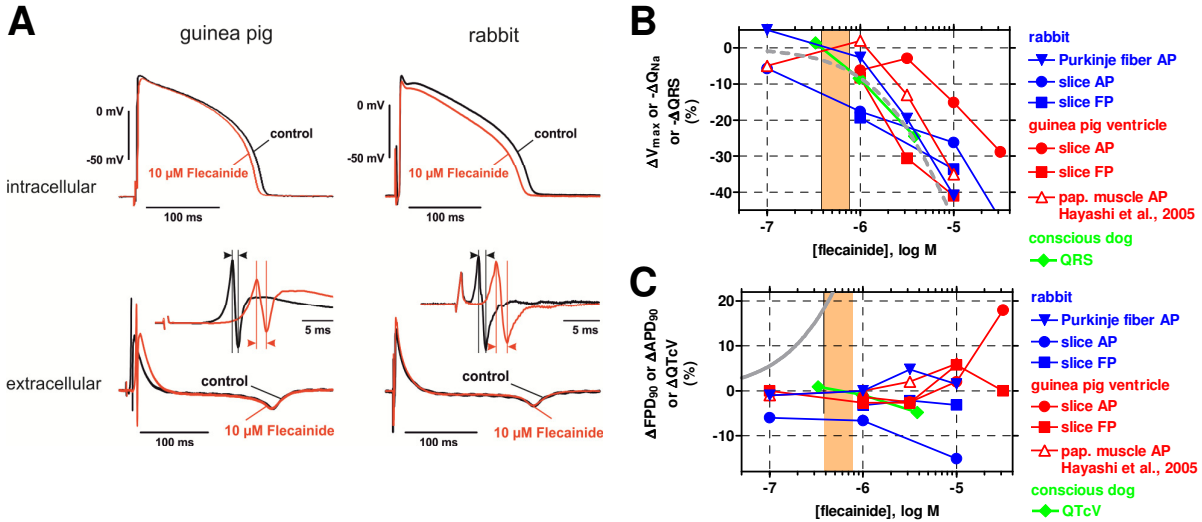


Fig. 1: **(A)** Examples of intracellular (action potential) and extracellular (field potential) recordings from guinea pig (left) and rabbit (right) ventricular slices. Shown are superimposed tracings before (pre-drug control; black) and following flecainide exposure (10 μM; red). Insets: enlarged view of primary and secondary peak of the FP, the latency difference (arrowheads) of which is a measure for Na<sup>+</sup> conductance ( $Q_{Na}$ ). **(B)** Concentration dependence of effects of flecainide on  $\Delta V_{max}$ ,  $\Delta Q_{Na}$ , and  $\Delta QRS$  in the following preparations: rabbit Purkinje fiber and ventricular slices, guinea pig ventricular slices and papillary muscle (data from Hayashi et al., 2005), and conscious dog. Also depicted is a concentration-response curve for inhibition of the hNav1.5 Na<sup>+</sup> current (dashed grey line) and the range of therapeutically effective protein-unbound drug plasma concentrations in humans (orange area; data from Redfern et al., 2003). Please note that throughout all figures (i) solid symbols reflect data originating from the authors laboratories, whereas data from the literature are depicted with unfilled symbols, and (ii) only mean values are depicted for clarity. **(C)** Concentration dependence of effects of flecainide on  $\Delta APD_{90}$ ,  $\Delta FPD_{90}$ , and  $\Delta QTcV$  in the following preparations: rabbit Purkinje fiber and ventricular slices, guinea pig ventricular slices and papillary muscle (data from Hayashi et al., 2005), and conscious dog. Also depicted is a concentration-response curve for inhibition of the hERG K<sup>+</sup> current (solid grey line) and the range of therapeutically effective protein-unbound drug plasma concentrations in humans (orange area; data from Redfern et al., 2003).

	hERG K <sup>+</sup> current		hNav1.5 Na <sup>+</sup> current		L-type Ca <sup>++</sup> current
	own IC <sub>50</sub> <sup>a</sup> (μmol/L)	literature IC <sub>50</sub> (μmol/L)	own IC <sub>50</sub> <sup>a</sup> (μmol/L)	literature IC <sub>50</sub> (μmol/L)	literature IC <sub>50</sub> (μmol/L)
flecainide	1.7	0.7-3.9 <sup>b</sup>	11	2.5-7 <sup>h</sup>	20, 41, 63 <sup>m</sup>
quinidine	N/A	0.41 <sup>c</sup>	12	20 <sup>i</sup>	10, 56 <sup>n</sup>
atenolol	>100	>1000 <sup>l</sup>	N/A	N/A	N/A
D,L-sotalol	1200	69 <sup>d</sup>	N/A	N/A	N/A
dofetilide	0.036	0.158 <sup>e</sup>	N/A	N/A	N/A
nifedipine	315	>50, 275 <sup>f</sup>	N/A	N/A	0.2-0.3 <sup>j</sup>
verapamil	0.68	0.143 <sup>g</sup>	N/A	N/A	1.0 <sup>k</sup>

Tab. 1: Effects of selected antiarrhythmics on hERG K<sup>+</sup> current, hNav1.5 Na<sup>+</sup> current, and cardiac L-type Ca<sup>++</sup> current in-vitro.

<sup>a</sup>largely unpublished IC<sub>50</sub> values from the laboratory of H.M.H. (D,L-sotalol IC<sub>50</sub> from Vormberge et al., 2006); N/A, not available; <sup>b</sup>Paul et al., 2002; Ducroq et al., 2007; <sup>c</sup>Paul et al., 2002; <sup>d</sup>Ducroq et al., 2007; Numaguchi et al., 2000; <sup>e</sup>Davie et al., 2004; Zhang et al., 1999; Zhabyayev et al., 2000; <sup>f</sup>Zhang et al., 1999; <sup>g</sup>estimated from Ducroq et al., 2007; Nitta et al., 1992; <sup>h</sup>estimated from Ducroq et al., 2007; <sup>i</sup>Uehara & Hume, 1985; Charnet et al., 1987; Shen et al., 2000; Zhang et al., 1999; Kawakami et al., 2006; <sup>j</sup>Scamps et al., 1989; Kihara et al., 1996; Hancox and Convery, 1997; <sup>k</sup>Scamps et al., 1989; Salata and Wasserstrom, 1988.

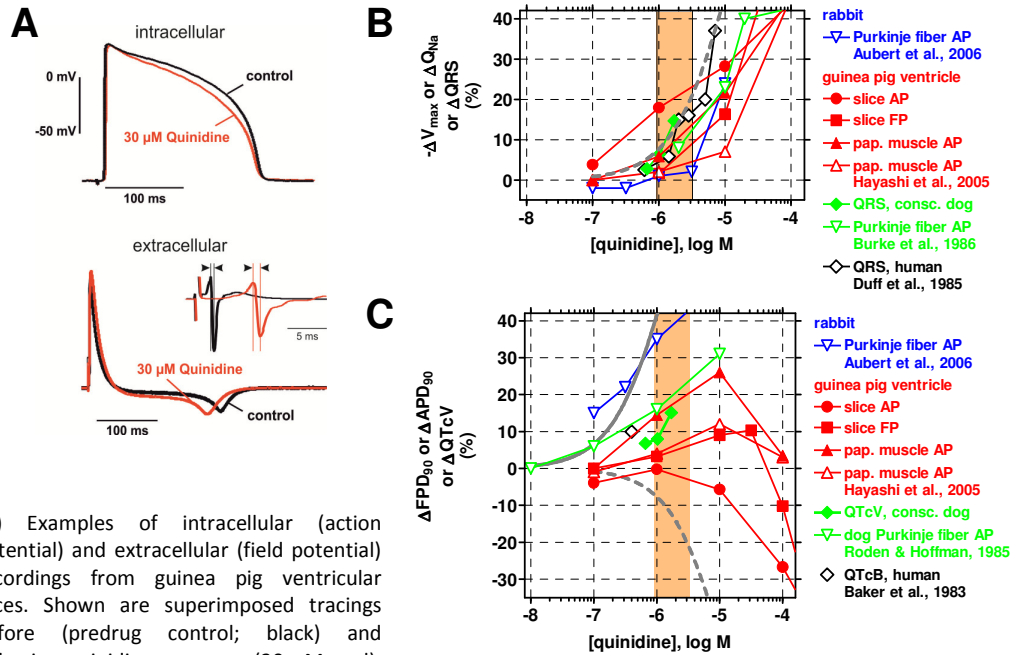


Fig. 2: **(A)** Examples of intracellular (action potential) and extracellular (field potential) recordings from guinea pig ventricular slices. Shown are superimposed tracings before (predrug control; black) and following quinidine exposure (30 μM; red). Insets: enlarged view of primary and secondary peak of the FP, the latency difference (arrowheads) of which is a measure for Na<sup>+</sup> conductance (Q<sub>Na</sub>). **(B)** Concentration dependence of effects of quinidine on  $\Delta V_{max}$ ,  $\Delta Q_{Na}$ , and  $\Delta QRS$  in the following preparations: rabbit Purkinje fiber (data from Aubert et al., 2006), guinea pig ventricular slices and papillary muscle (own data and data from Hayashi et al., 2005), conscious dog and dog Purkinje fiber (data from Burke et al., 1986), and human subjects (data from Duff et al., 1985). Also depicted is a concentration-response curve for inhibition of the hNav1.5 Na<sup>+</sup> current and the range of therapeutically effective protein-unbound drug plasma concentrations in humans (orange area; data from Redfern et al., 2003). **(C)** Concentration dependence of effects of quinidine on  $\Delta APD_{90}$ ,  $\Delta FPD_{90}$ , and  $\Delta QTcV$  in the following preparations: rabbit Purkinje fiber (data from Aubert et al., 2006), guinea pig ventricular slices and papillary muscle (own data and data from Hayashi et al., 2005), conscious dog and dog Purkinje fiber (data from Roden and Hoffman, 1985), and human subjects (data from Baker et al., 1983). Also depicted are concentration-response curves for inhibition of the hERG K<sup>+</sup> current (solid grey line) and the hNav1.5 Na<sup>+</sup> current (dashed grey line), and the range of therapeutically effective protein-unbound drug plasma concentrations in humans (orange area; data from Redfern et al., 2003).

## Results

### Class-1 antiarrhythmics flecainide and quinidine

As expected for Class-1 antiarrhythmics, both flecainide and quinidine are inhibitors of the human cardiac sodium channel hNav1.5 with IC<sub>50</sub> concentrations of 11 and 12 μM, respectively (Table 1, Figures 1B and 2B), and 20% inhibition at around 3 μM. At lower concentrations, however, quinidine and flecainide (IC<sub>50</sub> ~1.7 μM) also inhibit the hERG K<sup>+</sup> channel (Table 1, Figures 1C and 2C) with an IC<sub>20</sub> level at about 0.5 μM.

Because of this dual ion channel inhibition, flecainide and quinidine may interfere with both depolarisation and repolarisation, and hence the maximum rate of depolarisation, V<sub>max</sub>, of the cardiac action potential and its equivalent QNa in slices as well as APD and FPD are of particular interest. In guinea pig and rabbit ventricular slices (Table 3, Figures 1A+1B and 2A+2B), guinea pig papillary muscle (Table 2), and rabbit Purkinje fiber (Table 2, Figure 1B), V<sub>max</sub> is reduced and QNa is increased by both flecainide and quinidine with a concentration-dependence similar to that required for Na<sup>+</sup> current inhibition. When recording ECGs *in vivo*, Na<sup>+</sup> channel block manifests itself as slowing of conduction, i.e. widening of the QRS complex in the ECG. The corresponding effect is detected in

	rabbit Purkinje fiber action potential <sup>&amp;</sup>					guinea-pig papillary muscle action potential		
	concentration	V <sub>max</sub>	APD <sub>90</sub>	triangulation	-V <sub>max</sub>	V <sub>max</sub>	APD <sub>90</sub>	triangulation
	(μmol/L)	(V/s or Δ%)	(ms or Δ%)	(ms or Δ%)	(V/s or Δ%)	(V/s or Δ%)	(ms or Δ%)	(ms or Δ%)
flecainide N=4-6	0	393.0	445.3	124.0	-0.783			
	0.1	5.0	1.0	-2.9	-2.1			
	1	-2.6	0.0	44.5	-36.7			
	3	-19.6	-4.8	164.0	-65.7			
	10	-40.9	-1.5	257.1	-78.2			
quinidine N=6	0					153.2	158.8	58.7
	1					-5.8	14.5	1.7
	10					-21.6	26.0	21.0
	100					-59.0	3.5	12.4
atenolol N=5-6	0	259.4	475.7	135.5	-0.682			
	1	17.3	0.1	4.1	-6.3			
	10	4.3	-1.6	4.7	-6.7			
	100	8.5	-1.5	-0.8	-3.3			
D,L-sotalol N=5-6	0	273.4	331.8	116.2	-0.775	170.9	163.3	62.8
	1					-5.8	11.5	-4.7
	3	-21.4	6.1	-5.0	-4.9			
	10	-23.4	41.8	15.5	-18.2	-7.8	24.9	1.0
	30	2.9	119.0	127.9	-29.0	-7.4	29.6	36.6
dofetilide N=3-6	0	194.8	415.8	145.9	-0.772			
	0.3	-7.5	12.1	16.7	-12.2			
	1	-12.5	13.6	11.5	-15.0			
	3	-24.3	66.5	81.1	-42.7			
	10	-9.7	105.4	98.4	-57.7			
nifedipine N=5-7	0	318.0	447.3	77.4	-0.810			
	0.1	17.1	-3.8	-10.8	-0.9			
	1	-2.3	-8.9	19.8	8.5			
	10	7.1	-36.3	2.3	5.4			
verapamil N=4-6	0	305.8	397.3	80.3	-0.689			
	0.1	-1.7	-2.1	12.8	-13.3			
	1	5.7	11.5	31.1	-25.5			
	10	10.0	61.7	236.7	-61.7			

Tab. 2: Effects of selected antiarrhythmics on rabbit cardiac Purkinje fiber and guinea-pig papillary muscle action potential parameters in-vitro.<sup>§</sup>

§ Data are mean values from action potential measurements in rabbit Purkinje fibers and guinea pig papillary muscle; N refers to the number of preparations investigated (usually 1 preparation per animal). Pre-drug control values (concentration = 0) are absolute values in V s<sup>-1</sup> or ms, whereas all other values are expressed as percent change versus pre-drug control (Δ%). V<sub>max</sub>, maximal depolarisation velocity; APD<sub>90</sub>, action potential duration at 90% repolarisation; triangulation, difference between APD<sub>90</sub> and APD<sub>50</sub> (Purkinje fiber) or APD<sub>90</sub> and APD<sub>30</sub> (papillary muscle); -V<sub>max</sub>, maximal repolarisation velocity.

& Pre-drug control resting membrane potential in rabbit Purkinje fibers: flecainide, -88.7 ± 0.6 mV (mean ± SEM, N=6) [depolarization to -80.1 ± 3.4 mV at 10 μM]; quinidine, N/A; atenolol, -89.4 ± 0.5 mV (N=5); D,L-sotalol, -91.1 ± 1.4 mV (N=6); dofetilide, -90.5 ± 0.5 mV (N=6); nifedipine, -87.6 ± 0.4 mV (N=9); verapamil, -89.4 ± 0.5 mV (N=8). No major changes (i.e. > ± 3 mV) of resting membrane potential occurred throughout the experiments.

<b>A: guinea pig</b>		<b>action potential<sup>&amp;</sup></b>			<b>field potential</b>			
	concentration	V <sub>max</sub>	APD <sub>90</sub>	triangulation	-V <sub>max</sub>	Q <sub>Na</sub>	FPD	triangulation
	(μmol/L)	(V/s or Δ%)	(ms or Δ%)	(ms or Δ%)	(V/s or Δ%)	(ms or Δ%)	(ms or Δ%)	(ms or Δ%)
flecainide	0	162.7	180.2	36.8	N/A	0.9	190.8	N/A
N <sub>AP</sub> =12/5	1	-6.2	1.4	-0.3		8.3	2.7	
N <sub>FP</sub> =8/2	3	-2.9	2.5	-0.5		30.6	2.7	
	10	-15.1	-2.0	-3.3		41.0	-5.8	
quinidine	0	203.6	177.0	27.9	N/A	0.8	192.1	N/A
N <sub>AP</sub> =6/5	1	-15.2	0.27	6.0		1.6	9.0	
N <sub>FP</sub> =6/2	10	-25.1	-5.2	20.8		16.3	10.3	
	30					42.4	-10.2	
	100	-56.6	-28.7	11.2		79.7	-41.0	
atenolol	0	222.6	169.3	26.3	N/A	0.8	197.8	N/A
N <sub>AP</sub> =6/5	1	-14.7	-11.3	5.0		-1.2	1.9	
N <sub>FP</sub> =6/2	10	-21.7	-15.9	21.8		7.8	6.0	
	50					3.3	5.2	
D,L-sotalol	0	173.6	187.5	40.3	N/A	0.8	193.1	N/A
N <sub>AP</sub> =11/9	1	2.2	3.6	1.6		-2.3	-0.7	
N <sub>FP</sub> =9/2	3	0.7	5.3	3.6		5.9	3.5	
	10	3.5	12.1	14.3		4.9	12.0	
	30	3.4	18.2	28.4		-6.2	22.7	
	100	12.5	19.3	48.7			25.0	
dofetilide	0	181.1	178.4	25.9	N/A	0.9	202.4	N/A
N <sub>AP</sub> =7/4	0.001	1.1	2.4	2.3			9.2	
N <sub>FP</sub> =7/2	0.01	-0.4	13.1	17.3			10.2	
	0.1	-7.3	22.7	34.0		-1.2	20.8	
	1	-4.2	21.7	32.7		4.2	48.6	
nifedipine	0	138.2	178.2	27.9	N/A	1.0	212.3	N/A
N <sub>AP</sub> =8/4	0.1	-3.6	-2.8	-4.6		-1.2	-3.9	
N <sub>FP</sub> =8/2	1	-1.5	-16.9	-8.2		4.2	-26.3	
	10	7.7	-30.9	-15.0		5.8	-62.9	
verapamil	0	220.4	173.2	25.9	N/A	0.9	193.9	N/A
N <sub>AP</sub> =7/3	0.1	-15.3	-3.5	-1.3		-5.3	-5.6	
N <sub>FP</sub> =7/2	1	-6.3	-8.7	2.1		-17.3	-6.9	
	10	-7.0	-23.1	11.7		-11.1	-22.4	

<b>B: rabbit</b>		<b>action potential<sup>&amp;</sup></b>			<b>field potential</b>			
	concentration	V <sub>max</sub>	APD <sub>90</sub>	triangulation	-V <sub>max</sub>	Q <sub>Na</sub>	FPD	triangulation
	(μmol/L)	(V/s or Δ%)	(ms or Δ%)	(ms or Δ%)	(V/s or Δ%)	(ms or Δ%)	(ms or Δ%)	(ms or Δ%)
flecainide	0	170.9	182.0	52.3	N/A	0.9	183.9	N/A
N <sub>AP</sub> =6/2	0.1	-3.9	-2.8	0.2				
N <sub>FP</sub> =4/2	1	-9.6	-3.8	0.7		19.4	-3.2	
	3					33.6	-2.2	
	10	-16.9	-2.9	4.0		30.9	-3.1	
	30	-54.7	-17.7	-5				
dofetilide	0	139.0	215.8	46.4	N/A	0.7	192.6	N/A
N <sub>AP</sub> =4/2	0.001	0.0	6.5	2.5		-5.0	4.1	
N <sub>FP</sub> =4/2	0.01	-6.6	45.1	40.8		-5.3	18.4	
	0.1	-5.8	201.3	88.6		2.3	23.1	
nifedipine	0	141.7	215.7	36.3	N/A	0.9	211.7	N/A
N <sub>AP</sub> =3/2	0.1	11.7	-4.1	4.9		5.1	0.4	
N <sub>FP</sub> =4/2	1	3.1	-9.3	7.0		-3.4	-14.4	
	10	-1.7	-19.6	42.5		-0.7	-43.4	

conscious dogs (Table 4, Figures 1B and 2B), with a concentration dependence and to an extent similar to those required for Na<sup>+</sup> current inhibition.

Although flecainide is a potent inhibitor of hERG (Table 1), it does not substantially alter APD<sub>90</sub> and/or FPD<sub>90</sub> in guinea pig and rabbit ventricular slices (Table 3, Figure 1C), guinea pig papillary muscle, and rabbit Purkinje fiber (Table 2, Figure 1C), unless at concentrations ≥10 μM. Also QTcV in conscious dogs *in vivo* remains essentially unchanged (Table 4, Figure 1C) at concentrations overlapping and exceeding the human therapeutic range. It should be pointed out, however, that flecainide dramatically alters the shape of action potentials, particularly in rabbit Purkinje fibers, where the maximal repolarisation velocity is reduced and significant triangulation is observed (Table 2).

The results situation is more complex with quinidine, since there is considerable variation between types of tissue preparation and species. Concentration dependent APD<sub>90</sub> prolongation only is observed in rabbit Purkinje fibers (Lu et al., 2001; Aubert et al., 2006; Ducroq et al., 2007), at concentrations inhibiting hERG K<sup>+</sup> current (Figure 2C). In guinea pig papillary muscle, APD<sub>90</sub> is prolonged at ≤ 10 μM, while at ≥ 10 μM APD<sub>90</sub> returns to baseline (Table 2, Figure 2C; Hayashi et al., 2005). In guinea pig ventricular slices, FPD<sub>90</sub> is prolonged at ≤30 μM and shortened at higher concentrations, whereas APD<sub>90</sub> is only shortened at ≥ 10 μM (Table 3, Figure 2C). In conscious dogs, quinidine is associated with QTcV prolongation (Table 4, Figure 2C).

## Class-2 antiarrhythmic atenolol

The class-2 antiarrhythmic drug atenolol lacks any relevant interactions with cardiac ion channels, e.g. the hERG K<sup>+</sup> channel (Table 1), and this is also reflected by the fact that atenolol hardly alters the shape of cardiac action or field potentials. This is demonstrated in guinea pig ventricular slices (Figure 3, Table 3) and in rabbit Purkinje fiber (Table 2, Figure 3). In the former preparation, however, atenolol is associated with a concentration dependent shortening of the APD<sub>90</sub> in the range of 5-15%. Finally, *in vivo*, atenolol prolongs the PQ interval (lowered heart rate) but is without effect on the duration of the QTc interval in conscious dogs (Table 4, Figure 3B) at concentrations overlapping and exceeding the human therapeutic range (Figure 3B).

## Class-3 antiarrhythmics D,L-sotalol and dofetilide

The characteristic feature of class-3 antiarrhythmics is their ability to delay cardiac repolarisation as for instance by inhibition of the hERG K<sup>+</sup> channel by D,L-sotalol and dofetilide, with IC<sub>20</sub> concentrations of about 20 μM and 10 nM, respectively (Table 1, Figures 4B and 5B). In guinea pig ventricular slice preparations, the effect of D,L-sotalol is characterised by a concentration dependent drug-mediated prolongation of APD<sub>90</sub> and FPD<sub>90</sub>, the extent of which is approximately 20% at 30 μM

---

### Previous page

**Tab. 3:** Effects of selected antiarrhythmics on action potential and field potential parameters from guinea pig (A) and rabbit (B) ventricular slice preparations *in vitro*.<sup>§</sup>

**§** Data are mean values from action potential and field potential measurements in guinea pig and rabbit ventricular slice preparations; NAP=i/j refers to the number of slices used for AP measurements with i slices from j animals (the same applies to field potential (FP) measurements). Nomenclature analogous to Table 2; Q<sub>Na</sub>, latency difference between primary and secondary peak of the FP as measure for Na<sup>+</sup> conductance; FPD, field potential duration.

**&** Predrug control resting membrane potential in guinea pig and rabbit ventricular slices. Guinea pig: flecainide, -82.4 ± 1.5 mV (mean ± SEM, N=12); quinidine, -88.3 ± 2.5 mV (N=6); atenolol, -87.2 ± 2.5 mV (N=6); D,L-sotalol, -86.9 ± 1.3 mV (N=11); dofetilide, -88.4 ± 1.1 mV (N=7); nifedipine, -88.2 ± 2.9 mV (N=8); verapamil, -87.4 ± 1.8 mV (N=7). Rabbit: flecainide, -84.9 ± 1.4 mV (N=6); dofetilide, -91.7 ± 1.3 mV (N=5); nifedipine, -90.2 ± 2.8 mV (N=3). No major changes (i.e. > ± 3 mV) of resting membrane potential occurred throughout the experiments.

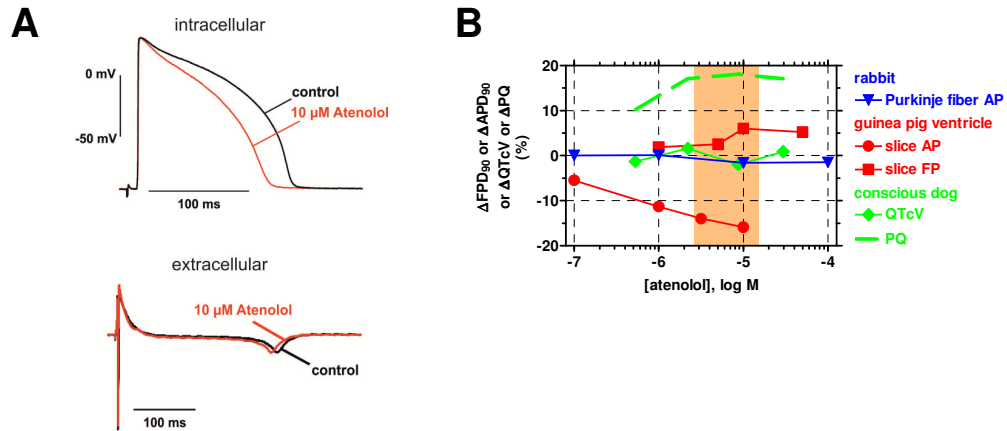


Fig. 3: **(A)** Examples of intracellular (action potential) and extracellular (field potential) recordings from guinea pig ventricular slices. Shown are superimposed tracings before (predrug control; black) and following atenolol exposure (10  $\mu$ M; red). **(B)** Concentration dependence of effects of atenolol on  $\Delta$ APD<sub>90</sub>,  $\Delta$ FPD<sub>90</sub>,  $\Delta$ QTcV and  $\Delta$ PQ in the following preparations: rabbit Purkinje fiber, guinea pig ventricular slices, and conscious dog. Also depicted is the range of therapeutically effective protein-unbound drug plasma concentrations in humans (orange area; data from Redfern et al., 2003).

(Table 3, Figure 4). A similar concentration dependence of APD<sub>90</sub> prolongation is observed in guinea pig papillary muscle (Table 2; Figure 4B), whereas rabbit Purkinje fibers are more sensitive to D,L-sotalol mediated APD prolongation (Table 2; Figure 4B). *In vivo*, D,L-sotalol prolongs the QT interval as demonstrated in conscious and anesthetized dogs at plasma concentrations and to an extent that are similar to the findings in guinea pig ventricular slices and to hERG K<sup>+</sup> current inhibition (Table 4, Figure 4B).

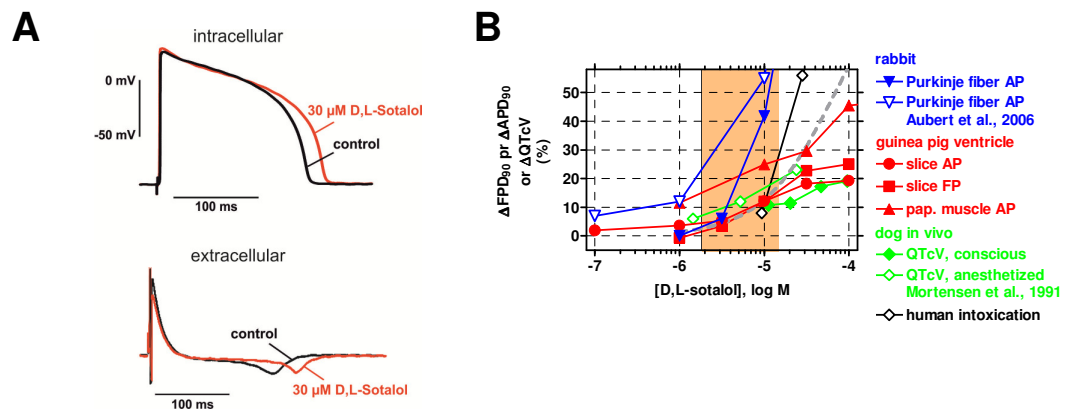


Fig. 4: **(A)** Examples of intracellular (action potential) and extracellular (field potential) recordings from guinea pig ventricular slices. Shown are superimposed tracings before (predrug control; black) and following D,L-sotalol exposure (30  $\mu$ M; red). **(B)** Concentration dependence of effects of D,L-sotalol on  $\Delta$ APD<sub>90</sub>,  $\Delta$ FPD<sub>90</sub>, and  $\Delta$ QTcV in the following preparations: rabbit Purkinje fiber (own data and data from Aubert et al., 2006), guinea pig ventricular slices and papillary muscle, conscious dog and anaesthetized dog (data from Mortensen et al., 1991). Also depicted is a concentration-response curve for inhibition of the hERG K<sup>+</sup> current (dashed grey line; data from Ducroq et al., 2007), and the range of therapeutically effective protein-unbound drug plasma concentrations in humans (orange area; data from Redfern et al., 2003).

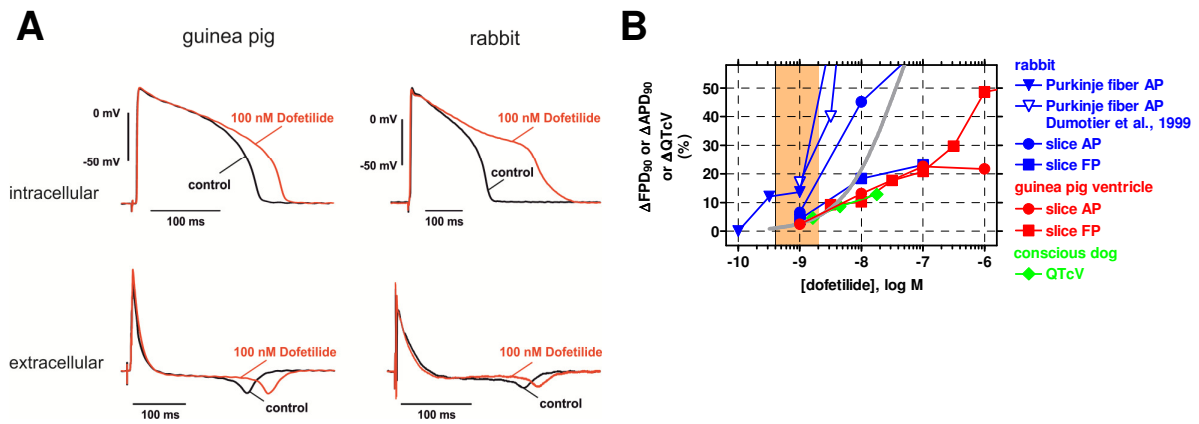


Fig. 5: **(A)** Examples of intracellular (action potential) and extracellular (field potential) recordings from guinea pig (left) and rabbit (right) ventricular slices. Shown are superimposed tracings before (predrug control; black) and following dofetilide exposure (100 nM; red). **(B)** Concentration dependence of effects of dofetilide on  $\Delta APD_{90}$ ,  $\Delta FPD_{90}$ , and  $\Delta QTcV$  in the following preparations: rabbit Purkinje fiber (own data and data from Dumotier et al., 1999) and ventricular slices, guinea pig ventricular slices, and conscious dog. Also depicted are a concentration-response curve for inhibition of the hERG  $K^+$  current (solid grey line) and the range of therapeutically effective protein-unbound drug plasma concentrations in humans (orange area; data from Redfern et al., 2003).

In a similar manner, the effect of dofetilide in both guinea pig and rabbit ventricular slice preparations is characterised by a concentration dependent drug-mediated prolongation of  $APD_{90}$  and  $FPD_{90}$ , the extent of which is approximately 20% at 10-30 nM (Table 3, Figure 5). Also here, rabbit Purkinje fibers are more sensitive towards dofetilide mediated APD or FPD prolongation (Table 2; Figure 5B). *In vivo*, dofetilide prolongs the QT interval in conscious dogs at plasma concentrations and to an extent that are similar to the findings in ventricular slice preparations and to hERG  $K^+$  current inhibition (Table 4, Figure 5B).

### Class-4 antiarrhythmics nifedipine and verapamil

The class-4 antiarrhythmics nifedipine and verapamil inhibit L-type calcium channels at submicromolar concentrations (Table 1, Figures 6B and 7B). In addition, both drugs are inhibitors of the hERG  $K^+$  channel (Table 1), albeit with one important difference. Nifedipine is a very low potency hERG blocker displaying an  $IC_{50}$  of about 3 orders of magnitude higher than that for calcium channel inhibition, whereas verapamil inhibits both hERG  $K^+$  and L-type calcium channel at almost identical concentrations (Table 1, Figures 6B and 7B).

The effects of nifedipine on the shape of cardiac action and field potentials are characterised by concentration dependent shortening of the  $APD_{90}$  and/or  $FPD_{90}$  in guinea pig and rabbit ventricular slices (Figure 6; Table 3), and rabbit Purkinje fibers (Table 2, Figure 6B) and a decrease in the AP plateau potential (Figure 6A); AP upstroke or  $Q_{Na}$  remains unaffected (Tables 2 and 3). The extent of APD/FPD shortening is similar in guinea pig slices, rabbit slices, and rabbit Purkinje fibers, and amounts to approximately 10-25% at 1  $\mu$ M. In contrast, the diastolic blood pressure in conscious dogs (Table 4, Figure 6B) is decreased to a similar extent already at approximately 3 orders of magnitude lower concentrations. At these low single-digit nanomolar concentrations, the QTcV interval in conscious dogs is not prolonged, but rather slightly shortened (Table 4, Figure 6B).

In guinea pig ventricular slice preparations, the effect of verapamil is characterised by a concentration dependent decrease in  $APD_{90}$  and  $FPD_{90}$  (Figure 7; Tables 2 and 3) with a magnitude of approximately 20% decrease at 10  $\mu$ M. In contrast, concentration dependent verapamil-mediated  $APD_{90}$  prolongation together with pronounced triangulation prevails in rabbit Purkinje fibers (Table

		BPS	BPD	HR	QRS	PQ	QT	QTcV	C <sub>max</sub>	C <sub>max,u</sub>
		mmHg	mmHg	bpm	ms	ms	ms	ms	μg/L	μmol/L
		Δ%								
flecainide (mg/kg)	BL	129	76	76	45	114	234	253	--	--
	3	+1.1	+3.9	+13.0	-1.4	-2.8	-2.9	+0.9	238	0.33
	10	-8.4	-1.0	+20.6	+8.4	+4.0	-5.1	-0.9	693	0.97
	30	+6.9	+23.7	+49.3	+24.5	+15.5	-8.7	-4.8	2700	3.78
quinidine (mg/kg)	BL	127	75	78	46	116	234	253	--	--
	5	-14.4	-15.9	+24.9	+2.8	-9.9	+4.1	+6.8	1631	0.65
	15	-15.5	-13.8	+39.3	+6.4	-10.8	+2.7	+8.0	2538	1.02
	45	-21.5	-18.4	+58.4	+14.7	-11.7	+2.6	+15.1	4229	1.69
atenolol (mg/kg)	BL	129	75	76	49	117	237	254	--	--
	0.3	-7.3	-9.3	-5.9	-0.4	+10.2	+0.4	-1.3	144	0.52
	1.5	-6.2	-6.1	-11.2	+1.3	+17.1	+5.3	+1.6	594	2.16
	5	-2.5	-5.1	-12.6	-1.5	+18.1	+1.7	-2.0	2388	8.70
	15	-6.9	-8.6	-10.1	+3.8	+17.1	+4.2	+0.9	8069	29.39
D,L-sotalol (mg/kg)	BL	134	83	85	51	110	234	259	--	--
	5	-4.5	-8.2	-12.6	+1.3	+14.9	+13.2	+10.7	3073	11.28
	10	-10.3	-9.9	+3.8	+3.2	+15.9	+4.2	+11.4	5533	20.31
	25	-18.9	-24.9	-10.9	+2.5	+18.8	+17.5	+17.2	12767	46.87
	50	-18.2	-15.5	+3.6	+2.1	+14.2	+16.3	+19.1	26302	96.56
dofetilide (mg/kg)	BL	133	78	88	48	108	227	255	--	--
	0.01	+0.1	-3.1	+1.4	+1.7	-2.5	+4.9	+4.6	1.55	0.0016
	0.03	+9.8	+4.9	-13.5	+2.0	+3.2	+13.6	+8.6	4.24	0.0044
	0.1	-2.9	-2.1	-6.7	-0.3	+11.6	+16.5	+12.8	16.90	0.0176
nifedipine (mg/kg)	BL	130	78	85	43	112	228	253	--	--
	0.3	-6.6	-9.8	-4.0	+2.6	+4.9	+1.4	+0.3	16	0.0002
	1	-15.7	-16.9	+36.1	+1.7	-6.5	-8.5	-1.0	53	0.0006
	3	-20.6	-24.0	+90.4	-6.2	-16.2	-18.2	-3.5	177	0.0020
verapamil (mg/kg)	BL	127	78	82	48	117	233	255	--	--
	3	-3.4	-4.3	+8.9	+3.3	+5.5	-0.1	+0.7	16	0.005
	10	-4.4	-2.6	+17.4	+1.7	+20.8	-3.7	-1.3	149	0.049
	20	-12.5	-10.5	+36.1	-3.3	+30.8	-5.9	+0.5	872	0.288

Tab. 4: Effects of selected antiarrhythmics on hemodynamic and ECG parameters in conscious, telemetry device-implanted Beagle dogs in-vivo.<sup>§</sup>

§ Data are mean values (N=5-6 per dose) of the following hemodynamic and ECG parameters: BPD, diastolic blood pressure; BPS, systolic blood pressure; HR, heart rate; QTcV, QT interval corrected for heart rate according to Van de Water. Predrug baseline values (BL) are absolute values in mmHg or bpm or ms, whereas all other values are expressed as percent change versus predrug baseline levels (Δ%). Maximal drug plasma concentrations (C<sub>max</sub>) were determined in satellite animals (N=3-4 per dose) and corrected for protein binding (C<sub>max,u</sub>). The following data (MW, molecular weight; fu, protein unbound fraction) was used to calculate C<sub>max,u</sub> values: flecainide: MW 414.3, fu 58% (human: [Zordan et al., 1993](#)); quinidine: MW 324.4, fu 13% (dog: [Rakhit et al., 1984](#)); atenolol: MW 266.3, fu 97% (human: Drug Information); D,L-sotalol: MW 272.4, fu 100% (dog: [Schnelle et al., 1973](#)); dofetilide: MW 441.6, fu 46% (dog: [Smith et al., 1992](#)); nifedipine: MW 346.3, fu 4% (dog: Bayer internal data); verapamil: MW 454.6, fu 15% (dog: [Belpaire et al., 1989](#)).

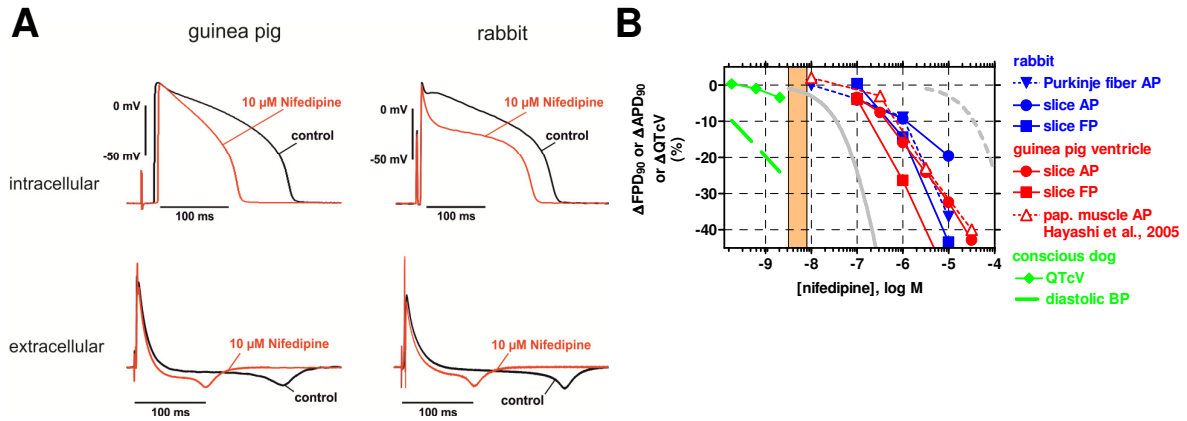


Fig. 6: **(A)** Examples of intracellular (action potential) and extracellular (field potential) recordings from guinea pig (left) and rabbit (right) ventricular slices. Shown are superimposed tracings before (predrug control; black) and following nifedipine exposure (10  $\mu$ M; red). **(B)** Concentration dependence of effects of nifedipine on  $\Delta$ APD<sub>90</sub>,  $\Delta$ FPD<sub>90</sub>, and  $\Delta$ QTcV in the following preparations: rabbit Purkinje fiber and ventricular slices, guinea pig ventricular slices and papillary muscle (data from Hayashi et al., 2005), and conscious dog. Also depicted are concentration-response curves for inhibition of the hERG K<sup>+</sup> current (dashed grey line) and the L-type Ca<sup>2+</sup> current (solid grey line; from Uehara and Hume, 1985), and the range of therapeutically effective protein-unbound drug plasma concentrations in humans (orange area; data from Redfern et al., 2003). The decrease in diastolic blood pressure (BP) in conscious dogs is also shown (solid green line).

2, Figure 7B). In conscious dogs, verapamil prolongs the PQ interval at concentrations that are about 1 order of magnitude lower than those associated with AP/FP duration changes *in vitro*, while the QTc interval duration is hardly affected within the same concentration range (Table 4, Figure 7B).

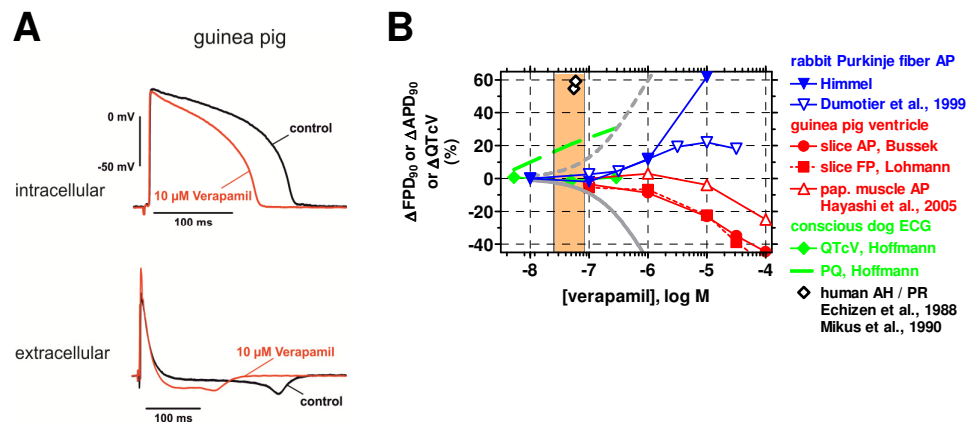


Fig. 7: **(A)** Examples of intracellular (action potential) and extracellular (field potential) recordings from guinea pig ventricular slices. Shown are superimposed tracings before (predrug control; black) and following verapamil exposure (10  $\mu$ M; red). **(B)** Concentration dependence of effects of verapamil on  $\Delta$ APD<sub>90</sub>,  $\Delta$ FPD<sub>90</sub>, and  $\Delta$ QTcV in the following preparations: rabbit Purkinje fiber (own data and data from Dumotier et al., 1999), guinea pig ventricular slices and papillary muscle (data from Hayashi et al., 2005), conscious dog, and human subjects (Echizen et al., 1988; Mikus et al., 1990). Also depicted are concentration-response curves for inhibition of the hERG K<sup>+</sup> current (dashed grey line) and the L-type Ca<sup>2+</sup> current (from Zhang et al., 1999), and the range of therapeutically effective protein-unbound drug plasma concentrations in humans (orange area; data from Redfern et al., 2003).

## Discussion

### Class-1 antiarrhythmics flecainide and quinidine

Quinidine and flecainide have been used in past decades in order to suppress/prevent ventricular tachyarrhythmias in humans (quinidine: [Halkin et al., 1979](#); [Carliner et al., 1980](#); [Rosen and Wit, 1983](#); [Duff et al., 1985](#); flecainide: [Duff et al., 1981](#); [Lui et al., 1982](#); [Hodges et al., 1982](#); [Estes et al., 1984](#)). Later, the proarrhythmic potential of these Class-1 antiarrhythmic drugs came more into focus ([Morganroth and Horowitz, 1984](#)) and led to investigations of the underlying electrophysiological mechanism(s).

Both flecainide and quinidine are inhibitors of the human cardiac sodium channel hNav 1.5 as demonstrated here (Table 1, Figures 1B and 2B) and as expected from the literature ([Hondegheem and Katzung, 1977](#); [Snyders and Hondegheem, 1990](#); [Konzen et al., 1990](#); [Nitta et al., 1992](#); [Ducroq et al., 2007](#)). At slightly lower concentrations, however, quinidine and flecainide also inhibit the hERG K<sup>+</sup> channel (Table 1, Figures 1C and 2C; [Paul et al., 2002](#); [Ducroq et al., 2007](#)), and at higher concentrations, both drugs interfere with other K<sup>+</sup> channels ([Slawsky and Castle, 1994](#)) and with L-type Ca<sup>2+</sup> channels (Table 1).

As expected for hNav 1.5 blockers, the maximum rate of depolarisation,  $V_{max}$ , of the cardiac action potential is reduced by flecainide and quinidine with a concentration dependence similar to that required for Na<sup>+</sup> current inhibition. This has been demonstrated in numerous ex-vivo action potential measurements, e.g. in preparations of rabbit Purkinje fiber (Table 2, Figure 1B and 2B; [Konzen et al., 1990](#); [Aubert et al., 2006](#)), dog Purkinje fiber ([Burke et al., 1986](#)), guinea pig papillary muscle (Table 2, Figure 1B; [Hayashi et al., 2005](#)), and guinea pig ventricular slices (Table 3, Figures 1B and 2B). In an *in vivo* situation, Na<sup>+</sup> channel block manifests itself as slowing of conduction, i.e. widening of the QRS complex in the ECG. The respective effect was detected in dogs (Table 4, Figures 1B and 2B; [Toyoshima et al., 2005](#); [Tashibu et al., 2005](#)) and in humans (flecainide: [Duff et al., 1981](#); [Lui et al., 1982](#); [Hodges et al., 1982](#); [Estes et al., 1984](#); [Conrad and Ober, 1984](#); quinidine: [Henning and Nyberg, 1973](#); [Halkin et al., 1979](#); [Carliner et al., 1980](#); [Duff et al., 1985](#)) in the same range of drug concentrations that cause hNav 1.5 inhibition and  $V_{max}$  decrease, and that overlap with the range of therapeutically effective protein-unbound drug plasma concentrations in humans ([Redfern et al., 2003](#)). As an equivalent to a prolonged QRS complex in the ECG following Na<sup>+</sup> channel blockade, the increase in the latency difference between the primary and the secondary peak of the FP ( $Q_{Na}$ ) indicates reduced Na<sup>+</sup> conductance in cardiac slices (Table 3; Figure 1A+1B and 2A+2B). In fact, both flecainide and quinidine increased  $Q_{Na}$  at concentrations that induce QRS widening *in vivo* (compare Tables 3 and 4).

Drugs that are highly selective blockers of the hERG K<sup>+</sup> channel are expected to prolong the duration of action/field potentials and the QT interval, whereas with mixed ion channel blockers such as flecainide and quinidine the net effect on APD, FPD, and QT is more difficult to predict. Despite being a potent inhibitor of hERG (Table 1, Figure 1C), flecainide does not substantially alter APD<sub>90</sub>/FPD<sub>90</sub> in rabbit Purkinje fiber (Table 2, Figure 1C), guinea pig and rabbit ventricular slices (Table 3, Figure 1A and 1C) and papillary muscle ([Hayashi et al., 2005](#)) unless at concentrations  $\geq 10$   $\mu$ M (Figure 1C; [Ducroq et al., 2007](#)). There, flecainide prolongs APD in guinea pig ventricular slices, but shortens it in rabbit ventricular slices; this might be explained by a differential contribution of L-type Ca<sup>2+</sup> channels to the shape of the ventricular slice AP, contributing more current in guinea pig and less in rabbit. Also QTcV in conscious dogs *in vivo* remains essentially unchanged (Table 4, Figure 1C) at concentrations overlapping and exceeding the human therapeutic range ([Redfern et al., 2003](#)). Finally, in rabbit Purkinje fibers, flecainide reduces the maximal repolarisation velocity resulting in significant triangulation (Table 2), whereas in ventricular preparations such a dramatic alteration of the shape of action potentials is not observed. The most likely reason for this difference is that the Purkinje fiber AP plateau depends to a greater extent on Na<sup>+</sup> and Ca<sup>2+</sup> influx than that of ventricular muscle.

Quinidine presents us with a more complex picture, since there is considerable variation between types of tissue preparation and species. Concentration dependent APD<sub>90</sub> prolongation only is observed in rabbit Purkinje fibers (Lu et al., 2001; Aubert et al., 2006; Ducroq et al., 2007), at concentrations inhibiting hERG K<sup>+</sup> current (Figure 2C). In guinea pig papillary muscle, APD<sub>90</sub> is prolonged at ≤ 10 μM, while at ≥ 10 μM APD<sub>90</sub> returns to baseline (Table 2, Figure 2C; Jurevicius et al., 1991; Hayashi et al., 2005). In guinea pig ventricular slices, FPD<sub>90</sub> is prolonged at ≤30 μM and shortened at higher concentrations, whereas APD<sub>90</sub> is only shortened at ≥ 10 μM (Table 3, Figure 2C). Overall, the prolongation of APD and FPD at lower quinidine concentrations in guinea pig ventricular preparations is consistent with the inhibition of repolarising hERG K<sup>+</sup> currents, while at higher quinidine concentrations the additional inhibition of depolarising L-type Ca<sup>2+</sup> currents (Table 1) shifts the balance towards an APD/FPD shortening. In conscious dogs, quinidine is associated with QTcV prolongation (Table 4, Figure 2C) occurring at similar magnitude as APD/FPD increases in the range of therapeutically effective protein-unbound drug plasma concentrations in humans (Figure 2C; Baker et al., 1983; Redfern et al., 2003). In dog Purkinje fibers, however, quinidine has been reported to mediate concentration dependent APD<sub>90</sub> prolongation (Figure 2C; Roden and Hoffman, 1985; Davidenko et al., 1989; Nemeth et al., 1997; Lu et al., 2001) as well as APD<sub>90</sub> shortening (Figure 2C; Burke et al., 1986) and even a biphasic effect (Wyse et al., 1993). This latter variability cannot be explained based on differential inhibition of depolarising versus repolarising ion channels, but may be due to differences in experimental protocols.

In general, the effects of multichannel blockers like flecainide or quinidine on action potential shapes are difficult to predict. For flecainide, blocking effects on I<sub>Kr</sub>, I<sub>Kur</sub>, I<sub>to</sub>, and I<sub>Ca</sub> have been reported. Since the contribution of individual channels to a certain AP shape shows large variations depending on species and location within the heart of one species, the effects of drugs like flecainide and quinidine will depend on the predominating conductance(s) during plateau or repolarisation phase and how they are affected by overlapping active concentration ranges (Dumotier et al., 1999), thus resulting in APD prolongation as well as shortening.

### Class-2 antiarrhythmic atenolol

For several decades, atenolol and other Class-2 antiarrhythmics have been among the mainstay drugs for treatment of heart failure and hypertension, and are known to possess few adverse effects, particularly with regard to proarrhythmia, and to improve life expectancy. The rather benign profile of atenolol is based on the lack of relevant interactions with cardiac ion channels including the hERG K<sup>+</sup> channel (Table 1; Kawakami et al., 2006), and is also reflected by the fact that atenolol hardly alters the shape of cardiac action potentials. This has been demonstrated in rabbit Purkinje fiber (Table 2, Figure 3B) and papillary muscle (Manley et al., 1986), and in guinea pig ventricular slices (Figure 3, Table 3). In the latter preparation, however, atenolol was associated with a concentration dependent shortening of the APD<sub>90</sub> which is considered most likely as “rundown” of the preparation. Finally, in the *in vivo* situation, atenolol prolonged the PQ interval (lowered heart rate) but was without effect on the duration of the QTc interval in conscious dogs (Table 4, Figure 3B; McAinsh and Holmes, 1983; Davies and McAinsh, 1986; Coppi et al., 1987; Kvetina et al., 1999) and human volunteers and patients (Coppi et al., 1987; Way et al., 1988; Demolis et al., 1997) and even in case of human intoxication (Snook et al., 2000).

### Class-3 antiarrhythmics D,L-sotalol and dofetilide

Class-3 antiarrhythmics had been developed with the specific aim to prolong the refractory period by prolonging the action potential duration, this being the main distinguishing feature compared to Class-1 antiarrhythmics. The electrophysiological basis of the delayed cardiac repolarisation is

inhibition of the hERG K<sup>+</sup> channel by D,L-sotalol and dofetilide (Table 1, Figures 4 and 5; Numaguchi et al., 2000; Davie et al., 2004; Ducroq et al., 2007). This is in line with concentration dependent drug-mediated prolongation of APD<sub>90</sub> and FPD<sub>90</sub> in the following ex-vivo preparations: rabbit Purkinje fiber (Table 2, Figures 4B and 5B; Abrahamsson et al., 1993; Dumotier et al., 1999; Lu et al., 2001, 2002; Aubert et al., 2006; Ducroq et al., 2007) and papillary muscle (Manley et al., 1986; Abrahamsson et al., 1993), dog Purkinje fiber (Knilians et al., 1991; Gwilt et al., 1991; Wyse et al., 1993; Lee et al., 1996; Nemeth et al., 1997; Lu et al., 2001) and papillary muscle (Nemeth et al., 1997), guinea pig papillary muscle (Table 2, Figure 4B; Tande et al., 1990; Davie et al., 2004), and guinea pig ventricular slices (Table 3, Figures 4 and 5). *In vivo*, both D,L-sotalol and dofetilide prolong the QT interval as demonstrated in conscious (Table 4, Figures 4B and 5B; Schneider et al., 2005) and anaesthetised dogs (Mortensen et al., 1991; Tashibu et al., 2005; Vormberge et al., 2006) as well as in human patients (Wang et al., 1986; Way et al., 1988; Redfern et al., 2003) or intoxications (Elonen et al., 1979; Neuvonen et al., 1981; Wang et al., 1986; Edvardsson and Varnauskas, 1997).

Although the direction of drug-induced changes is consistent throughout the various models in general, there is considerable variation in terms of sensitivity when individual models and species are compared. The magnitude of effects as well as the D,L-sotalol sensitivity of models is comparable for inhibition of the hERG K<sup>+</sup> current, prolongation of APD<sub>90</sub>/FPD<sub>90</sub> in guinea pig papillary muscle and ventricular slices, and prolongation of the QTc interval in anaesthetised and conscious dogs (Figure 4B); there, the 20% effect concentrations cluster mostly in the range between 10 and 100 μM (Figure 4B). In contrast, both effect size and sotalol sensitivity appear to be greater in rabbit and dog Purkinje fibers and in humans since concentration-response curves are steeper and shifted to approximately 10-fold lower concentrations (Figure 4B). The picture is similar for dofetilide (Figure 5B) where 20% prolongation of APD<sub>90</sub> in rabbit and dog Purkinje fibers occurs in the single digit nanomolar range and overlaps with human therapeutically effective protein-unbound plasma concentrations. For hERG K<sup>+</sup> current inhibition, APD<sub>90</sub>/FPD<sub>90</sub> prolongation in rabbit, dog, and guinea pig ventricular muscle, and QTcV prolongation in conscious dogs, however, double digit nanomolar dofetilide concentrations are required to reach the 20% effect level. In addition, rabbit appears to be the most and guinea pig the least sensitive species, regardless of whether this rank order is established for Purkinje fiber or for ventricular muscle preparations. Literature reports point into the same direction with regard to (i) a differential species sensitivity of Purkinje fibers towards delayed repolarisation (e.g.: Lu et al., 2001), and (ii) a higher sensitivity of Purkinje fibers versus ventricular muscle towards the APD shortening or prolonging effects of sodium channel or hERG K<sup>+</sup> channel blockers (e.g.: Abrahamsson et al., 1996 [rabbit]; Lathrop, 1985 [dog]) because of quantitative differences of the underlying ionic currents (e.g.: Cordeiro et al., 1998 [rabbit]). Another important point of discussion concerns a potential bias introduced by sex-specific differences in ventricular repolarisation (for review see: Cheng, 2006). Females are more sensitive towards APD prolongation than males, particularly at extremely low stimulation rates, as demonstrated in rabbit Purkinje fiber (Lu et al., 2000) and Langendorff heart (Liu et al., 1998), and in human patients and volunteers (Lehmann et al., 1999; Somberg et al., 2011), whereas this issue remains controversial in guinea pig ventricle (Hreiche et al., 2009; Brouillette et al., 2007) and in canine ventricle (Xiao et al., 2006). Also inward currents vary with sex and cardiac region as shown for the L-type calcium current (Sims et al., 2008).

#### Class-4 antiarrhythmics nifedipine and verapamil

Both nifedipine and verapamil share the common feature of Class-4 antiarrhythmics, i.e. they inhibit L-type calcium channels at submicromolar concentrations (Table 1, Figures 6B and 7B; Uehara and Hume, 1985; Charnet et al., 1987; Zhang et al., 1999; Shen et al., 2000). However, since the potency of nifedipine is markedly increased at depolarised potentials, nifedipine targets predominantly the L-type calcium channels modulating vascular smooth muscle tone, whereas the main therapeutic effect

of verapamil is to delay atrioventricular conduction. In addition, both drugs are inhibitors of the hERG  $K^+$  channel. However, nifedipine has a very low potency of about 3 orders of magnitude beyond that of calcium channel inhibition, thus physiologically irrelevant, whereas verapamil inhibits both hERG  $K^+$  and L-type calcium channel at almost identical concentrations (Table 1, Figures 6B and 7B; Zhang et al., 1999; Zhabyayev et al., 2000).

Since nifedipine is a fairly selective calcium channel blocker, its effects on the shape of cardiac action potentials are straightforward and characterised by concentration dependent shortening of the  $APD_{90}/FPD_{90}$  in rabbit Purkinje fibers (Table 2, Figure 6B; Dumotier et al., 1999), dog Purkinje fibers (Lee et al., 1996), cat and guinea pig papillary muscle (Bayer et al., 1977; Jurevicius et al., 1991; Hayashi et al., 2005), and guinea pig and rabbit ventricular slices (Table 3, Figure 6). This  $APD_{90}$  shortening is observed at concentrations approximately 2-3 orders of magnitude higher than those required to decrease the diastolic blood pressure in conscious dogs (Table 4, Figure 6B) or the range of therapeutically effective protein-unbound drug plasma concentrations in man (Redfern et al., 2003). Due the functional antagonism of hERG  $K^+$  and L-type calcium channel block and consistent with the *in vitro/ex-vivo* findings, the QTcV interval in conscious and anaesthetised dogs is not prolonged, but rather slightly shortened (Table 4, Figure 6B; Amlie et al., 1979; Tashibu et al., 2005). Whenever nifedipine-induced QTc prolongation is reported, the actual consensus opinion attributes this to an inadequate heart rate correction of the QT interval (e.g. Toyoshima et al., 2005).

The well-balanced mixed ion channel blocker verapamil presents a decidedly different picture, since the effect on  $APD_{90}/FPD_{90}$  in *ex vivo* preparations ranges from prolongation to shortening, obviously depending on the type of preparation (Tables 2 and 3, Figure 7B). Concentration dependent verapamil-mediated  $APD_{90}$  prolongation prevails in canine (Cranfield et al., 1974; Rosen et al., 1974) and rabbit Purkinje fibers (Table 2, Figure 7B; Dumotier et al., 1999), whereas in guinea pig papillary muscle (Zhang et al., 1997; Hayashi et al., 2005) or ventricular slices (Table 3, Figure 7) rather  $APD_{90}$  shortening is observed. The desired effect of PQ interval prolongation occurs in conscious and anaesthetised dogs within the same concentration range as the therapeutic effect in man (Table 4, Figure 7B; Shiina et al., 2000; Echizen et al., 1988; Mikus et al., 1990; Redfern et al., 2003), while the QTc interval duration is hardly affected, adequate heart rate correction provided (Table 4, Figure 7B; Shiina et al., 2000; Fossa et al., 2002; Schneider et al., 2005; Toyoshima et al., 2005; Tashibu et al., 2005).

## Limitations and opportunities

Similar to other multicellular preparations, it is conceivable that neurotransmitters are released due to field stimulation also in cardiac tissue slices. In our preparation, we have used a small concentric stimulation electrode which is expected to minimise the effect of electrical stimulation on neurotransmitter release. This problem, however, has not yet been addressed systematically by inhibiting neurotransmitter release or by blocking neurotransmitter effects.

In cardiac slice preparations it might reasonably be expected that drug actions on fibroblasts could be an area of considerable interest or matter of concern (Porter and Turner, 2009). Fibroblasts within cardiac tissue are assumed to play an important role in bridging electrical activity between myocytes. Since fibroblasts are coupled to myocytes by connexins (MacCannell et al., 2007), drug interaction with connexins but also interactions with fibroblast ion channels might influence drugs effects on the cardiac action potential. Investigating such an interaction was beyond the scope of our present work, and we are also not aware of publications addressing this question. We believe that these putative interactions have to be studied on isolated fibroblasts and in co-culture with cardiac myocytes. Although the tissue architecture in cardiac slice preparations is in principle not different from that of other multicellular preparations, cardiac slices may be more readily accessible for the study of specific modulation of fibroblast characteristics by gene transfer and/or knock down methods.

## Conclusion

In this paper, we have presented integrated data regarding electrophysiological effects of selected antiarrhythmic drugs (flecainide, quinidine, atenolol, sotalol, dofetilide, nifedipine, verapamil) using complementary *in vitro* and *in vivo* study types. These complementary approaches range from measurement of membrane currents (hERG,  $I_{Na}$ ,  $I_{Ca,L}$ ), to action/field potential in slices, Purkinje fiber action potential, and hemodynamic/ECG parameters (conscious dog), and also include published data. The main result of this complementary approach is that field and action potential recordings from heart slices correlate well with established *in vitro* and *in vivo* models in terms of pharmacology and predictability. Heart slice preparations yield similar results as papillary muscle but offer enhanced throughput for mechanistic investigations, and reduce the use of laboratory animals.

## Acknowledgements and Author Contributions

The expert technical assistance of Manuela Weisflog and Waldemar Hink (heart slice action potential), Susanne Herbold (voltage clamp), Marcus Deitermann (Purkinje fiber action potential), and Thomas Vormberge (conscious dog model) is gratefully acknowledged. This work was supported by the German Federal Ministry for Economy and Technology BMWi (PRO INNO II program, grant KF0682501 SB8 to A.B., E.W., M.S., and H.L.). Finally, the authors would like to thank Michael Kayser and Dr. Frank Thorsten Hafner (Bioanalytics, Bayer Pharma) for measuring drug plasma concentrations.

Major contributions by the authors to this work were as follows: (1) conception and design (HMH, HL, EW); (2) collection and assembly of data: voltage clamp experiments (HMH), rabbit Purkinje fiber action potential recordings (HMH), guinea pig papillary muscle action potential recordings (RB), ventricular slice action and field potentials recordings (AB, EW, MS, HL), studies in conscious dogs (MH), and literature search (HMH); (3) data analysis and interpretation (HMH, AB, EW, MS, HL, MH, RB); (4) manuscript writing (HMH).

## References

- Abrahamsson C, Carlsson L, Duker G (1996). Lidocaine and nisoldipine attenuate almokalant-induced dispersion of repolarisation and early afterdepolarisations *in vitro*. *J Cardiovasc Electrophysiol* **7**: 1074-1081.
- Abrahamsson C, Duker G, Lundberg C, Carlsson L (1993). Electrophysiological and inotropic effects of H-234/09 (almokalant) *in vitro* - A comparison with 2 other novel  $I_K$  blocking drugs, UK-68,798 (dofetilide) and E-4031. *Cardiovasc Res* **27**: 861-867.
- Alexander SPH, Mathie A, Peters JA (2009). Guide to Receptors and Channels (GRAC), 4<sup>th</sup> edition (2009). *Br J Pharmacol* **158 (Suppl. 1)**: S1-S254.
- Amlie JP, Refsum H, Landmark K (1979). The effect of nifedipine on the monophasic action potential and refractoriness of the right ventricle of the dog heart *in situ* after beta adrenergic receptor blockade. *Acta Pharmacol Toxicol (Copenh)* **44**: 185-90.
- Anon. (2005). ICH S7B: The nonclinical evaluation of the potential for delayed ventricular repolarisation (QT interval prolongation) by human pharmaceuticals. <http://www.ich.org/products/guidelines/safety/article/safety-guidelines.html>.
- Aubert M, Osterwalder R, Wagner B, Parrilla I, Cavero I, Doesseger L *et al.* (2006). Evaluation of the rabbit Purkinje fiber assay as an *in vitro* tool for assessing the risk of drug-induced Torsades de Pointes in humans. *Drug Safety* **29**: 237-254.
- Baker BJ, Gammill J, Massengill J, Schubert E, Karin A, Doherty JE (1983). Concurrent use of quinidine and disopyramide: evaluation of serum concentrations and electrocardiographic effects. *Am Heart J* **105**: 12-5.

- Barclay CJ (2005). Modelling diffusive O<sub>2</sub> supply to isolated preparations of mammalian skeletal and cardiac muscle. *J Muscle Res Cell Motil* **26**: 225-235.
- Bayer R, Rodenkirchen R, Kaufmann R, Lee JH, Hennekes R (1977). The effects of nifedipine on contraction and monophasic action potential of isolated cat myocardium. *Naunyn-Schmiedeberg's Arch Pharmacol* **301**: 29-37.
- Belpaire FM, De Rick A, De Smet F, Bourda A, Rosseel MT, Bogaert MG (1989). Influence of lidocaine on plasma protein binding and pharmacokinetics of verapamil in dogs. *Prog Clin Biol Res* **300**: 437-40.
- Brouillette J, Lupien MA, St-Michel C, Fiset C (2007). Characterization of ventricular repolarisation in male and female guinea pigs. *J Mol Cell Cardiol* **42**: 357-366.
- Burke GH, Loukides JE, Berman ND (1986). Comparative electropharmacology of mexiletine, lidocaine and quinidine in a canine Purkinje fiber model. *J Pharmacol Exp Ther* **237**: 232-6.
- Bussek A, Wettwer E, Christ T, Lohmann H, Camelliti P, Ravens U (2009). Tissue slices from adult mammalian hearts as a model for pharmacological drug testing. *Cell Physiol Biochem* **24**: 527-536.
- Carliner NH, Fisher ML, Crouthamel WG, Narang PK, Plotnick GD (1980). Relation of ventricular premature beat suppression to serum quinidine concentration determined by a new and specific assay. *Am Heart J* **100**: 483-9.
- Charnet P, Quadid H, Richard S, Nargeot J (1987). Electrophysiological analysis of the action of nifedipine and nicardipine on myocardial fibers. *Fundam Clin Pharmacol* **1**: 413-431.
- Cheng J (2006). Evidences of the gender-related differences in cardiac repolarisation and the underlying mechanisms in different animal species and human. *Fund Clin Pharmacol* **20**: 1-8.
- Colbert CM (2006). Preparation of cortical brain slices for electrophysiological recording. *Methods Mol Biol* **337**: 117-125.
- Conrad GJ, Ober RE (1984). Metabolism of flecainide. *Am J Cardiol* **53**: 41B-51B.
- Coppi G, Mosconi P, Springolo V (1987). Pharmacokinetics of a fixed combination of atenolol and indapamide in dogs and humans after oral administration. *Curr Ther Res* **42**: 411- 18.
- Cordeiro JM, Spitzer KW, Giles WR (1998). Repolarising K<sup>+</sup> currents in rabbit heart Purkinje cells. *J Physiol* **508**: 811-823.
- Cranefield PF, Aronson RS, Wit AL (1974). Effect of verapamil on the normal action potential and on a calcium-dependent slow response of canine cardiac Purkinje fibers. *Circ Res* **34**: 204-13.
- Davidenko JM, Cohen L, Goodrow R, Antzelevitch C (1989). Quinidine-induced action potential prolongation, early afterdepolarisations, and triggered activity in canine Purkinje fibers. Effects of stimulation rate, potassium, and magnesium. *Circulation* **79**: 674-86.
- Davie C, Valentin JP, Pollard C, Standen N, Mitcheson J, Alexander P *et al.* (2004). Comparative pharmacology of guinea pig cardiac myocyte and cloned hERG (I-Kr) channel. *J Cardiovasc Electrophysiol* **15**: 1302-1309.
- Davies MK, McAinsh J (1986). Tissue atenolol levels following chronic beta-adrenoceptor blockade using oral atenolol in dogs. *J Pharm Pharmacol* **38**: 316-9.
- Demolis JL, Martel C, Funck-Brentano C, Sachse A, Weimann HJ, Jaillon P (1997). Effects of tedisamil, atenolol and their combination on heart and rate-dependent QT interval in healthy volunteers. *Br J Clin Pharmacol* **44**: 403-409.
- Ducroq J, Printemps R, Guilbot S, Gardette J, Salvétat C, Le Grand M (2007). Action potential experiments complete hERG assay and QT-interval measurements in cardiac preclinical studies. *J Pharmacol Toxicol Methods* **56**: 159-170.
- Duff HJ, Roden DM, Maffucci RJ, Vesper BS, Conard GJ, Higgins SB *et al.* (1981). Suppression of resistant ventricular arrhythmias by twice daily dosing with flecainide. *Am J Cardiol* **48**: 1133-40.
- Duff HJ, Wyse DG, Manyari D, Mitchell LB (1985). Intravenous quinidine: relations among concentration, tachyarrhythmia suppression and electrophysiologic actions with inducible sustained ventricular tachycardia. *Am J Cardiol* **55**: 92-97.
- Dumotier BM, Adamantidis MM, Puisieux FL, Bastide MM, Dupuis BA (1999). Repercussions of pharmacologic reduction in ionic currents on action potential configuration in rabbit Purkinje fibers: Are they indicative of proarrhythmic potential? *Drug Dev Res* **47**: 63- 76.
- Echizen H, Manz M, Eichelbaum M (1988). Electrophysiologic effects of dextro- and levoverapamil on sinus node and AV node function in humans. *J Cardiovasc Pharmacol* **12**: 543-6.
- Edvardsson N, Varnauskas E (1987). Clinical course, serum concentrations and elimination rate in a case of massive sotalolol intoxication. *Eur Heart J* **8**: 544-8.
- Edwards FA, Konnerth A, Sakmann B, Takahashi T (1989). A thin slice preparation for patch clamp recordings from neurones of the mammalian central nervous system. *Pflügers Arch* **414**: 600-612.

- Elonen E, Neuvonen PJ, Tarssanen L, Kala R (1979). Sotalol intoxication with prolonged QT interval and severe tachyarrhythmias. *Br Med J* **1** (6172): 1184.
- Estes NA, Garan H, Ruskin JN (1984). Electrophysiologic properties of flecainide acetate. *Am J Cardiol* **53**: 26B-29B.
- Fossa AA, Depasquale MJ, Raunig DL, Avery MJ, Leishman DJ (2002). The relationship of clinical QT prolongation to outcome in the conscious dog using a beat-to-beat QT-RR interval assessment. *J Pharmacol Exp Ther* **302**: 828-833.
- Gwilt M, Arrowsmith JE, Blackburn KJ, Burges RA, Cross PE, Dalrymple HW *et al.* (1991). UK-68,798: a novel, potent and highly selective class III antiarrhythmic agent which blocks potassium channels in cardiac cells. *J Pharmacol Exp Ther* **256**: 318-24.
- Halkin H, Vered Z, Millman P, Rabinowitz B, Neufeld HN (1979). Steady-state serum quinidine concentration: role in prophylactic therapy following acute myocardial infarction. *Isr J Med Sci* **15**: 583-7.
- Hamill OP, Marty A, Neher E, Sakmann B, Sigworth FJ (1981). Improved patch-clamp techniques for high-resolution current recording from cells and cell-free membrane patches. *Pflügers Arch*, **391**: 85-100.
- Hancox JC, Convery MK (1997). Inhibition of L-type calcium current by flecainide in isolated single rabbit atrioventricular nodal myocytes. *Exp Clin Cardiol* **2**: 163-170.
- Hanton G, Nahas K, Priou C, Rabemampianina Y, Baneux P (2001). The QT Interval in the Dog ECG: Importance in Preclinical Toxicology and Relationship to Heart Rate. *Toxicology Method*, **11**: 21-40.
- Hayashi S, Kii Y, Tabo M, Fukuda H, Itoh T, Shimosato T *et al.* (2005). QT PRODACT: A multi-site study of *in vitro* action potential assays on 21 compounds in isolated guinea pig papillary muscles. *J Pharmacol Sci* **99**: 423-437.
- Henning R, Nyberg G (1973). Serum quinidine levels after administration of three different quinidine preparations. *Eur J Clin Pharmacol* **6**: 239-44.
- Himmel HM, Hoffmann M (2010). QTc shortening with a new investigational cancer drug: a brief case study. *J Pharmacol Toxicol Methods* **62**: 72-81
- Himmel HM (2007). Suitability of commonly used excipients for electrophysiological *in vitro* safety pharmacology assessment of effects on hERG potassium current and on rabbit Purkinje fiber action potential. *J Pharmacol Toxicol Methods* **56**: 145-158.
- Hodges M, Haugland JM, Granrud G, Conard GJ, Asinger RW, Mikell FL *et al.* (1982). Suppression of ventricular ectopic depolarisations by flecainide acetate, a new antiarrhythmic agent. *Circulation* **65**: 879-85.
- Hondeghem LM, Katzung BG (1977). Time- and voltage-dependent interactions of antiarrhythmic drugs with cardiac sodium channels. *Biochim Biophys Acta* **472**: 373-98.
- Hreiche R, Morisette P, Zakrzewski-Jakubiak, Turgeon J (2009). Gender-related differences in drug-induced prolongation of cardiac repolarisation in prepubertal guinea pigs. *J Cardiovasc Pharmacol Ther* **14**: 28-37.
- Jurevicius J, Muckus K, Macianskiene R, Chmel-Dunaj GN (1991). Influence of action potential duration and resting potential on effects of quinidine, lidocaine and ethmozine on Vmax in guinea pig papillary muscle. *J Mol Cell Cardiol* **23 (Suppl 1)**: 103-114.
- Kawakami K, Nagatomo T, Abe H (2006). Comparison of HERG channel blocking effects of various beta-blockers - implication for clinical strategy. *Br J Pharmacol* **147**: 642-652.
- Kihara Y, Inoko M, Hatakeyama N, Momose Y, Sasayama S (1996). Mechanisms of negative inotropic effects of class 1c antiarrhythmic agents: comparative study of the effects of flecainide and pilsicainide on intracellular calcium handling in dog ventricular myocardium. *J Cardiovasc Pharmacol* **27**: 42-51.
- Knilians TK, Lathrop DA, Nanasi PP, Schwartz A, Varro A (1991). Rate and concentration dependent effects of UK-68,798, a potent new class III antiarrhythmic, on canine Purkinje fibre action potential duration and Vmax. *Br J Pharmacol* **103**: 1568-72.
- Konzen G, Reichardt B, Hauswirth O (1990). Fast and slow blockade of sodium channels by flecainide in rabbit cardiac Purkinje fibres. *Naunyn Schmiedebergs Arch Pharmacol* **341**: 565-76.
- Kvetina J, Svoboda Z, Nobilis M, Pastera J, Anzenbacher P (1999). Experimental goettingen minipig and beagle dog as two species used in bioequivalence studies for clinical pharmacology (5-aminosalicylic acid and atenolol as model drugs). *Gen Physiol Biophys* **18 (Special Issue)**: 80- 85.
- Lathrop DA (1985) Electromechanical characterization of the effects of racemic sotalol and its optical isomers on isolated canine ventricular trabecular muscles and Purkinje strands. *Can J Physiol Pharmacol* **63**: 1506-1512.
- Lee HC, Cai JJ, Arnar DO, Shibata EF, Martins JB (1996). Mechanism of alpha-2 adrenergic modulation of canine Purkinje fiber action potential. *J Pharmacol Exp Ther* **278**: 597-606.

- Lehmann MH, Hardy S, Archibald D, MacNeil DJ (1999). JTC prolongation with d,l-sotalol in women versus men. *Am J Cardiol* **83**: 354-359.
- Liu YK, Katchman A, Drici MD, Ebert SN, Ducic I, Morad M, Woosley RL (1998). Gender difference in the cycle length-dependent QT and potassium currents in rabbits. *J Pharmacol Exp Ther* **285**: 672-679.
- Lu HR, Marien R, Saels A, De Clerck F (2000). Are there sex-specific differences in ventricular repolarisation or in drug-induced early afterdepolarisations in isolated rabbit Purkinje fibers? *J Cardiovasc Pharmacol* **36**: 132-139.
- Lu HR, Marien R, De Clerck F (2001). Species plays an important role in drug-induced prolongation of action potential duration and early afterdepolarisations in isolated Purkinje fibers. *J Cardiovasc Electrophysiol* **12**: 93-102.
- Lu HR, Vlamincx E, Van Ammel K, De Clerck F (2002). Drug-induced long QT in isolated rabbit Purkinje fibers: importance of action potential duration, triangulation and early afterdepolarisations. *Eur J Pharmacol* **452**: 183-192.
- Lui HK, Lee G, Dietrich P, Low RI, Mason DT (1982). Flecainide-induced QT prolongation and ventricular tachycardia. *Am Heart J* **103**: 567-9.
- Manley BS, Alexopoulos D, Robinson GJ, Cobbe SM (1986). Subsidiary class III effects of beta blockers? A comparison of atenolol, metoprolol, nadolol, oxprenolol and sotalol. *Cardiovasc Res* **20**: 705-9.
- McAinsh J, Holmes BF (1983). Pharmacokinetic studies with atenolol in the dog. *Biopharm Drug Dispos* **4**: 249-61.
- MacCannell KA, Bazzazi H, Chilton L, Shibukawa Y, Clark RB, Giles WR (2007). A mathematical model of electrotonic interactions between ventricular myocytes and fibroblasts. *Biophys J* **92**: 4121-4132.
- Mikus G, Eichelbaum M, Fischer C, Gumulka S, Klotz U, Kroemer HK (1990). Interaction of verapamil and cimetidine: stereochemical aspects of drug metabolism, drug disposition and drug action. *J Pharmacol Exp Ther* **253**: 1042-8.
- Morganroth J, Horowitz LN (1984). Flecaïnide: its proarrhythmic effect and expected changes on the surface electrocardiogram. *Am J Cardiol* **53**: 89B-94B.
- Mortensen E, Tande PM, Klow NE, Refsum H (1991). Plasma concentrations and hemodynamic effects of d-sotalol after beta-blockade in dogs. *Pharmacol Toxicol* **68**: 420-425.
- Nemeth M, Varro A, Virag L, Hala O, Thormaehlen D, Papp JG (1997). Frequency dependent Cardiac Electrophysiologic Effects of Tedisamil: Comparison With Quinidine and Sotalol. *J Cardiovasc Pharmacol Ther* **2**: 273-284.
- Neuvonen PJ, Elonen E, Vuorenmaa T, Laakso M (1981). Prolonged Q-T interval and severe tachyarrhythmias, common features of sotalol intoxication. *Eur J Clin Pharmacol* **20**: 85-9.
- Nitta J, Sunami A, Marumo F, Hiraoka M (1992). States and sites of actions of flecaïnide on guinea pig cardiac sodium channels. *Eur J Pharmacol* **214**: 191-197.
- Numaguchi H, Mullins FM, Johnson JP, (2000). Probing the interaction between inactivation gating and d-sotalol block of HERG. *Circ Res* **87**: 1012-1018.
- Parrish AR, Gandolfi AJ, Brendel K (1995). Precision-cut tissue slices: applications in pharmacology and toxicology. *Life Sci* **57**: 1887-1901.
- Paul AA, Witchel HJ, Hancox JC (2002). Inhibition of the current of heterologously expressed HERG potassium channels by flecaïnide and comparison with quinidine, propafenone and lignocaine. *Br J Pharmacol* **136**: 717-729.
- Porter KE, Turner NA (2009). Cardiac fibroblasts: at the heart of myocardial remodeling. *Pharmacol Ther* **123**: 255-278.
- Rakhit A, Holford NH, Effenev DJ, Riegelman S (1984). Induction of quinidine metabolism and plasma protein binding by phenobarbital in dogs. *J Pharmacokinetic Biopharm* **12**: 495-515.
- Redfern WS, Carlsson L, Davis AS, Lynch WG, MacKenzie I, Palethorpe S *et al.* (2003). Relationships between preclinical cardiac electrophysiology, clinical QT interval prolongation and torsade de pointes for a broad range of drugs: evidence for a provisional safety margin in drug development. *Cardiovasc Res* **58**: 32-45.
- Roden DM, Hoffman BF (1985). Action potential prolongation and induction of abnormal automaticity by low quinidine concentrations in canine Purkinje fibers. Relationship to potassium and cycle length. *Circ Res* **56**: 857-67.
- Rosen MR, Ilvento JP, Gelband H, Merker C (1974). Effects of verapamil on electrophysiologic properties of canine cardiac Purkinje fibers. *J Pharmacol Exp Ther* **189**: 414-22.
- Rosen MR, Wit AL (1983). Electropharmacology of antiarrhythmic drugs. *Am Heart J* **106**: 829-39.
- Salata JJ, Wasserstrom JA (1988). Effects of quinidine on action potentials and ionic currents in isolated canine ventricular myocytes. *Circ Res* **62**: 324-337.

- Scamps F, Undrovinas A, Vassort G (1989). Inhibition of ICa in single frog cardiac cells by quinidine, flecainide, ethmozin and ethazin. *Am J Physiol* **256**: C549-C559.
- Schneider J, Hauser R, Andreas JO, Linz K, Jahnel U (2005). Differential effects of human ether-a-go-go-related gene (HERG) blocking agents on QT duration variability in conscious dogs. *Eur J Pharmacol* **512**: 53-60.
- Schnelle K, Garrett ER (1973). Pharmacokinetics of the beta-adrenergic blocker sotalol in dogs. *J Pharmacol Sci* **62**: 362-75.
- Sellin LC, McArdle JJ (1994). Multiple effects of 2,3-butanedione monoxime. *Pharmacol Toxicol* **74**: 305-313.
- Shen JB, Jiang B, Pappano AJ (2000). Comparison of L-type calcium channel blockade by nifedipine and/or cadmium in guinea pig ventricular myocytes. *J Pharmacol Exp Ther* **294**: 562-570.
- Shiina H, Sugiyama A, Takahara A, Satoh Y, Hashimoto K (2000). Comparison of the electropharmacological effects of verapamil and propranolol in the halothane anesthetized *in vivo* canine model under monophasic action potential monitoring. *Jpn Circ J* **64**: 777-82.
- Sims C, Reisenweber S, Viswanathan PC, Choi BR, Walker WH, Salama G (2008). Sex, age, and regional differences in L-type calcium current are important determinants of arrhythmia phenotype in rabbit hearts with drug-induced long QT type 2. *Circ Res* **102**: e86-e100.
- Slawsky MT, Castle NA (1994). K<sup>+</sup> channel blocking actions of flecainide compared with those of propafenone and quinidine in adult rat ventricular myocytes. *J Pharmacol Exp Ther* **269**: 66-74.
- Smith DA, Rasmussen HS, Stopher DA, Walker DK (1992). Pharmacokinetics and metabolism of dofetilide in mouse, rat, dog and man. *Xenobiotica* **22**: 709-719.
- Snook CP, Sigvaldason K, Kristinsson J (2000). Severe atenolol and diltiazem overdose. *J Toxicol-Clin Toxicol* **38**: 661-665.
- Snyders DJ, Hondeghem LM (1990). Effects of quinidine on the sodium current of guinea pig ventricular myocytes. Evidence for a drug-associated rested state with altered kinetics. *Circ Res* **66**: 565-79.
- Somberg JC, Preston RA, Ranade V, Cvetanovic I, Molnar J (2011). Gender differences in cardiac repolarisation following intravenous sotalol administration. *J Cardiovasc Pharmacol Ther*, DOI: 10.1177/1074248411406505.
- Tande PM, Bjoernstad H, Yang T, Refsum H (1990). Rate-dependent class III antiarrhythmic action, negative chronotropy, and positive inotropy of a novel IK blocking drug, UK-68,798: potent in guinea pig but no effect in rat myocardium. *J Cardiovasc Pharmacol* **16**: 401-10.
- Tashibu H, Miyazaki H, Aoki K, Akie Y, Yamamoto K (2005). QT PRODACT: *In vivo* QT assay in anesthetized dog for detecting the potential for QT interval prolongation by human pharmaceuticals. *J Pharmacol Sci* **99**: 473-486.
- Toyoshima S, Kanno A, Kitayama T, Sekiya K, Nakai K, Haruna M *et al.* (2005). QT PRODACT: *in vivo* QT assay in the conscious dog for assessing the potential for QT interval prolongation by human pharmaceuticals. *J Pharmacol Sci* **99**: 459-471.
- Uehara A, Hume JR (1985). Interactions of organic calcium channel antagonists with calcium channels in single frog atrial cells. *J Gen Physiol* **85**: 621-647.
- Van de Water A, Verheyen J, Xhonneux R, Reneman RS (1989). An improved method to correct the QT interval of the electrocardiogram for changes in heart rate. *J Pharmacol Methods* **22**: 207-217.
- Vickers AE, Fisher RL (2004). Organ slices for the evaluation of human drug toxicity. *Chem Biol Interact* **150**: 87-96.
- Vormberge T, Hoffmann M, Himmel HM (2006). Safety pharmacology assessment of drug induced QT-prolongation in dogs with reduced repolarisation reserve. *J Pharmacol Toxicol Methods* **54**: 130-140.
- Wang T, Bergstrand RH, Thompson KA, Siddoway LA, Duff HJ, Woosley RL *et al.* (1986). Concentration-dependent pharmacologic properties of sotalol. *Am J Cardiol* **57**: 1160-5.
- Way BP, Forfar JC, Cobbe SM (1988). Comparison of the effects of chronic oral therapy with atenolol and sotalol on ventricular monophasic action potential duration and effective refractory period. *Am Heart J* **116**: 740-746.
- Wyse KR, Ye V, Campbell TJ (1993). Action potential prolongation exhibits simple dose dependence for sotalol, but reverse dose-dependence for quinidine and disopyramide –Implications for proarrhythmia due to triggered activity. *J Cardiovasc Pharmacol* **21**: 316-322.
- Xiao L, Zhang L, Han W, Wang Z, Nattel S (2006). Sex-based transmural differences in cardiac repolarisation and ionic-current properties in canine left ventricles. *Am J Physiol* **291**: H570-H580.
- Zhabiyev P, Missan S, Jones SE, McDonald TF (2000). Low-affinity block of cardiac K(+) currents by nifedipine. *Eur J Pharmacol* **401**: 137-143.

- Zhang S, Sawanobori T, Hirano Y, Hiraoka M (1997). Multiple modulations of action potential duration by different calcium channel blocking agents in guinea pig ventricular myocytes. *J Cardiovasc Pharmacol* **30**: 489-496.
- Zhang ST, Zhou ZF, Gong QM, Makielski JC, January CT (1999). Mechanism of block and identification of the verapamil binding domain to hERG potassium channels. *Circ Res* **84**: 989-998
- Zhou ZF, Gong Q, Ye B, Fan Z, Makielski JC, Robertson GA *et al.* (1998). Properties of hERG channels stably expressed in HEK293 cells studied at physiological temperature. *Biophys J* **74**: 230-241.
- Zordan R, Padrini R, Bernini V, Piovan D, Ferrari M (1993). Influence of age and gender on the *in vitro* serum protein binding of flecainide. *Pharmacol Res* **28**: 259- 264.